To the Graduate Council:

I am submitting herewith a thesis written by Alexander Page Davis-Smith entitled "Effect of Micro-Fabric on Consolidation Behavior of Reconstituted Kaolin Clay." I have examined the final electronic copy of this thesis for form and content and recommend that it be accepted in partial fulfillment of the requirements for the degree of Master of Science, with a major in Civil Engineering.

Dayakar Penumadu
Major Professor

We have read this thesis
and recommend its acceptance:

Edwin G. Burdette

Richard M. Bennett

Accepted for the Council:

Anne Mayhew
Vice Chancellor and
Dean of Graduate Studies

(Original signatures are on file with official student records.)

EFFECT OF MICRO-FABRIC ON CONSOLIDATION BEHAVIOR OF RECONSTITUTED KAOLIN CLAY

A Thesis Presented for the
Master's Degree
University of Tennessee, Knoxville

Alexander Page Davis-Smith
December 2004

ACKNOWLEDGMENTS:

I wish to thank all of my professors at the University of Tennessee in Knoxville. I especially wish to thank Dr. Penumadu for providing an environment in which I was able to do meaningful research. Dr. Bennett and Dr. Burdette are greatly appreciated for serving on my committee. The mentoring and technical support of Amit Prashant is also greatly acknowledged. I also wish to thank my family who supported me while I was in college.

Financial support from the National Science Foundation (NSF) through grants CMS-9872618 and CMS-0296111 is greatly acknowledged. Any opinions, findings, and conclusions or recommendations expressed in this material are those of the authors and do not necessarily reflect the views of NSF.

ABSTRACT:

The effect of micro-fabric (i.e. geometric arrangement of platelets) on the one-dimensional consolidation behavior of reconstituted kaolin clay is evaluated using a series of controlled-rate-of-strain (CRS) and incremental load (IL) consolidation tests. The causes and implications of changes in micro-fabric are also explored. Micro-fabric has been altered by adding a dispersing agent to the slurry during specimen preparation; and the changes in micro-fabric have been observed with scanning electron microscope (SEM) images and x-ray diffraction analysis. Properties of the pore fluid are found to affect micro-fabric, even in the presence of significant mechanical stresses. It is observed that the changes in micro-fabric significantly affect the compressibility of reconstituted kaolin clay in the normally consolidated zone. Samples with preferred platelet orientation and closer inter-platelet spacing are significantly less compressible than those with randomly oriented platelets. In the over-consolidated zone, the compressibility is not significantly affected by changes in micro-fabric, but the compressibility does depend on the direction in which stress is applied. Samples with preferred platelet orientation show more isotropic nature of consolidation properties than samples with randomly oriented platelets. The values of the virgin compression index (C_c) and swelling index (C_s) are observed to be higher when axial load is applied parallel to the direction of preferred platelet orientation. Anisotropy observed in the normally consolidated zone is mostly due to the elastic portion of the deformation.

KEY WORDS: Micro-fabric, Kaolin, Consolidation, Controlled-Rate-of-Strain, Flocculated, Dispersed, Anisotropy, SEM, X-ray Diffraction, Zeta Potential, Rheology, Compressibility.

TABLE OF CONTENTS:

Part 1: Experiments and Results 1

Section 1: Introduction 2

Section 2: Preparation of Specimens with Varying Micro-Fabric 5

Section 3: Observation of Changes in Micro-Fabric 8

Section 4: Effects of Dispersing Agent on Kaolin Clay Slurry 13

Section 5: Leeching Tests Performed under Applied Vertical Stress 17

Section 6: Controlled-Rate-of-Strain (CRS) Consolidation Testing 21

Section 7: Consolidation Testing Program and Data Analysis 26

Section 8: Consolidation Test Results 29

Section 9: Summary and Conclusions 37

Part 2: Recommendations for Modeling 42

Section 1: Recommendations for Quantifying Micro-Fabric 43

Section 2: Recommendations for Modeling One-Dimensional Consolidation 48

References 52

Appendix 1: Tables and Figures 58

Vita 76

LIST OF TABLES:

Table Page

1. Settling Column Test Results 59

2. Summary of Effects of Dispersing Agent on Slurry Properties 59

3. Summary of Leeching Tests under Applied Vertical Stress 59

4. Virgin Compression and Swelling Indexes 60

5. Degrees of Anisotropy 61

6. Degrees of Plasticity 61

LIST OF FIGURES:

Figure	Page
1. Consolidometer and Extruded Cubical Specimen	62
2. SEM Image of Air-Dried Sediment from Kaolin Clay Slurry Prepared	
(a) without a Dispersing Agent (10,000x) and	63
(b) with a Dispersing agent (25,000x)	63
3. Siemens Diffractometer model D500	64
4. X-ray Diffraction Pattern for Air-Dried Sediment from Kaolin Clay Slurry	
Prepared (a) without a Dispersing Agent and	65
(b) with Dispersing Agent	65
5. X-ray Diffraction Pattern for One-Dimensionally Consolidated	
(Preconsolidation Stress = 30 psi) Kaolin Clay Sample with	
(a) Flocculated Micro-Fabric and	66
(b) Dispersed Micro-Fabric	66
6. Diagram Explaining the Concept of Zeta Potential	67
7. Rheology Testing Apparatus and Cup and Bob Geometry	68
8. Rheology Test Results as a Function of Shear Rate for Kaolin Clay Slurry	
Prepared (a) without a Dispersing Agent	69
(b) with Dispersing Agent	69
9. Shear Stress as a Function of Shear Rate for Kaolin Clay Slurry	
Prepared (a) without a Dispersing Agent	70
(b) with Dispersing Agent	70
10. Diagram Explaining Orientation of Consolidation Test Samples Relative	

to their Orientation in the Consolidometer during Specimen Preparation 71

11. Disassembled Cell and Controlled-Rate-of-Strain (CRS) Consolidation Testing Apparatus with Computer and Data Acquisition System 72

12. Representative One-Dimensional Consolidation Curves for Vertical and Horizontal Kaolin Clay Samples with Flocculated and Dispersed Micro-Fabric 73

13. Comparison between CRS and IL Consolidation Test Results for
    (a) Flocculated Micro-Fabric and 74
    (b) Dispersed Micro-Fabric 74

14. Geometric Model Used to Obtain Effective Thickness (t_e) and Average Platelet Orientation Angle (θ) as a Function of Void Ratio 75

NOTATION:

Cc = virgin compression index, obtained from 1-D consolidation tests

Cch = virgin compression index of horizontal samples for a given micro-fabric

Ccv = virgin compression index of vertical samples for a given micro-fabric

Cs = swelling index, obtained from unloading portion of 1-D consolidation tests

Csh = swelling index of horizontal samples for a given micro-fabric

Csv = swelling index of vertical samples for a given micro-fabric

e = void ratio

e_d = with reference to a leeching test performed under a given vertical effective stress, the average void ratio of samples prepared with a dispersing agent under the same vertical effective stress

e_f = final void ratio in a given test (For tests performed in a settling column, this is the final void ratio of the sediment—after the addition of a dispersing agent to the supernatant fluid for leeching tests. For leeching tests performed under a given vertical effective stress, this is the final void ratio of the consolidated sample—after the addition of a dispersing agent to the surrounding water.)

e_o = initial void ratio in a given test (For tests performed in a settling column, this is the initial void ratio of the slurry. For tests performed in CRS or IL consolidation test setups, this is the initial void ratio of the consolidated sample.)

e_l = in leeching tests performed under an applied vertical effective stress, the void ratio under the vertical effective stress applied—before the addition of dispersing agent (For leeching tests performed in a settling column (zero vertical effective stress), this is the final void ratio of the sediment before the addition of a dispersing agent to the supernatant fluid. For tests performed in an IL consolidation test setup, this is the final void ratio of the consolidated sample under the applied vertical effective stress before the addition of a dispersing agent to the surrounding water.)

t_e = effective thickness (the average aspect ratio of arbitrary cross sections of platelets)

V_s = volume of solids

V_t = total volume

V_v = volume of voids

ΔV = change in volume

θ = average orientation angle of platelets relative to the preferred direction of platelet orientation, which is assumed to be perpendicular to the vertical axis or the axis of one-dimensional loading

θ_o = initial average orientation angle

PART ONE

EXPERIMENTS AND RESULTS

1. INTRODUCTION:

Evaluating the consolidation behavior of clay is important because the parameters obtained during consolidation tests are used to predict settlements when external loads are applied to clay deposits. Consolidation parameters also play an important role in representing the yield behavior for various constitutive models such as the modified Cam clay model (Roscoe and Burland 1968), MIT-E3 model (Whittle 1993; Whittle and Kavvadas 1994), and MIT-S1 model (Pestana and Whittle 1999; Pestana et al. 2002). This paper concentrates on the effect of micro-fabric on the one-dimensional consolidation properties and the associated anisotropy of kaolin clay. This study was carried out by preparing consolidation test samples with different micro-fabric using the same powdered kaolin clay so that the mechanical and geometric properties of the individual platelets could be assumed to be constant. The relationship between the electro-chemical properties of pore fluid in kaolin clay and micro-fabric is also explored. This research is important because different types of micro-fabric exist in nature (Penumadu 1996) and it is important to evaluate the variation of the void ratio-log of effective stress relationship for identical clay platelets with differing geometric arrangement in order to isolate the effect of changes in micro-fabric on the compressibility of a given type of clay.

The author is unaware of any research that has been done to experimentally quantify the effect of varying micro-fabric on consolidation behavior, but there has been extensive research on clay micro-fabric and structure in general (Bennett and Hurlbut 1986; Chen and Anandarajah 1998; Lambe 1958; Mitchell 1956; Quigley and Thompson 1966). Sensitivity of clay behavior to remolding has also been studied extensively, which is related to changes in micro-fabric and structure (Casagrande 1932; Liu et al. 2003; Terzaghi 1941). The findings presented in this study provide an experimental verification for the explanation of changes in natural clay behavior that are observed upon remolding that was given by Bennett and Hurlbut (1986). This explanation is called *the principal of chemical irreversibility of clay fabric* and supplements traditional explanations of clay sensitivity, which were in terms of cementation (Winterkorn and Tschebotarioff 1947).

It has been suggested (Lambe 1958; Mitchell 1956; Quigley and Thompson 1966; Terzaghi et al. 1996) that the application of high vertical stress without lateral strain causes platelets to arrange parallel to each other and perpendicular to the axis of loading. These changes in micro-fabric may be the cause of the decrease in the virgin compression index (*Cc*) that is sometimes observed at high vertical effective stresses (Terzaghi et al. 1996). The changes in micro-fabric could be incorporated into large strain consolidation theories such as those of Gibson et al. (1967, 1981). This quantification would be useful because, for example, Mesri and Olsen (1971) have noted that in addition to void ratio, permeability also depends on tortuosity of flow channels and void size distribution—which are both related to micro-fabric.

It is suggested that micro-fabric be quantified for modeling purposes in terms of the average angle of orientation of platelets relative to a plane perpendicular to the axis of rotational symmetry, which is typically the axis of one-dimensional loading. Penumadu (1996) describes a numerical method to obtain particle orientation histograms from scanning electron micrographs in order to quantitatively represent the micro-fabric of a sample. These polar histograms are easily translated into an average angle of platelet orientation. The procedure involves the use of a digital image analysis of scanning electron micrographs at appropriate magnification using an Intensity Gradient Analysis.

2. PREPARATION OF SPECIMENS WITH VARYING MICRO-FABRIC:

Changes in micro-fabric were achieved by adding a dispersing agent (sodium hexa-metaphosphate—commercially calgon) to the de-aired and de-ionized water used for slurry preparation prior to remolding. Kaolin clay platelets have a negative net surface charge on their face, but—in a low pH environment—a positive net charge on their edges (Lambe 1958; Mitchell 1993). When a dispersing agent such as sodium hexa-metaphosphate is added to kaolin clay slurry prior to remolding, negatively charged ions are introduced and adsorbed on the positively charged edges of the platelets. Therefore, the variation of surface charge (from positively charged edges to negatively charged faces) is removed or significantly reduced. In the absence of a dispersing agent, the edge of a given platelet is attracted to the faces of others, resulting in a "card-house" arrangement of platelets. If no external stress is applied, then the orientation angle of a given platelet in this case is approximately random. If a dispersing agent is added to the slurry and the variation of surface charge is removed, then all portions of the platelets repel each other and the agglomerations of platelets that are present in normal kaolin clay specimens will not exist. In this case, the platelets arrange themselves parallel to each other, causing a significantly lower initial void ratio for a given preconsolidation stress than would be reached without the addition of a dispersing agent. The direction of preferred platelet orientation is perpendicular to the direction of axial loading.

Two types of specimens with different micro-fabric were made from the same powdered kaolin clay using de-aired and de-ionized water according to the recommendations of Penumadu et al. (1998). The two types of micro-fabric are referred to as "flocculated" and "dispersed". For both types of specimens, powdered kaolin clay was added to de-aired, de-ionized water to yield a slurry water content of 155%. The slurry was then mixed using a high shear mixer for a constant duration in order to achieve uniformity. The specimens were then vertically consolidated under K_o conditions in a consolidometer with a square cross-section to form a cubical specimen. The preconsolidation stress of the consolidated specimens was 207 kPa (30 psi). The inside of the cubical base of the consolidometer was lined with Teflon and the inside of both the base and the extension had been sprayed with silicon to reduce friction during consolidation and extrusion. The consolidometer and an extruded cubical specimen are shown in Figure 1 (all figures and tables may be found in Appendix 1). When dispersed micro-fabric was desired, sodium hexa-metaphosphate was dissolved in the de-aired, de-ionized water to create a 2% solution prior to the addition of the powdered kaolin clay.

The amount of dispersing agent to be added was determined by Hazen and Penumadu (1999) by allowing the solids in slurries with varying concentrations of sodium hexa-metaphosphate (as well as other dispersing agents) to settle in 1000 mL graduated cylinders. The final height of the sediment was seen to be the smallest when a 2% solution of sodium hexa-metaphosphate was used as the pore fluid. This concentration of sodium hexa-metaphosphate was concluded to be that which caused the greatest amount of anisotropy of platelet arrangement (i.e. dispersion).

It should be noted that the specimens with the “dispersed micro-fabric” described in this study did have some agglomerations of platelets and all of the platelets are not perfectly parallel to each other. Therefore, it is not necessarily the theoretical limiting case. Furthermore, the specimens with the “flocculated micro-fabric” described in this study, which have essentially random platelet orientation, did have some anisotropy of platelet arrangement due to the one-dimensional stress that was applied in the consolidometer during specimen preparation. If, however, the platelets in slurry prepared without a dispersing agent were allowed to settle out of suspension and no external stress was applied, then purely random micro-fabric could be obtained. It is assumed that the stress-induced anisotropy due to the platelets self-weight would be negligible.

3. OBSERVATION OF CHANGES IN MICRO-FABRIC:

In clay slurry, platelets arrange themselves in the most stable configuration as dictated by electro-chemical attractive and repulsive forces—independently of external loads applied during remolding. For kaolin clay slurry with no dispersing agent added and no externally applied stress, this would be an essentially random arrangement of platelets. For kaolin clay slurry prepared with a dispersing agent, however, the most stable configuration is for all platelets to be parallel (because essentially all electro-chemical forces are repulsive). This is the configuration for which each point on any given plate is the farthest away from all other platelets as possible. An experiment was performed to quantify the effect of adding a dispersing agent in the absence of externally applied mechanical stress. Slurries were prepared with and without dispersing agent and poured into 1000 ml graduated cylinders and the solids were allowed to settle until the height of the sediment remained constant. The values of final void ratio (e_f) for sediments from slurries prepared with and without a dispersing agent are shown in Table 1. Since the slurry prepared without a dispersing agent only settled slightly, the process was repeated at twice the initial slurry water content. It should be noted that when the initial void ratio was doubled, the final void ratio of the sediment was greater than the initial void ratio of normal slurry. The significant difference in the values for final void ratio of the sediments from slurries prepared with and without a dispersing agent implies that the micro-fabric was already defined by electro-chemical forces even though the platelets had not been subjected to any effective stress beyond their own self-weight.

This concept was verified with scanning electron microscope (SEM) images. Slurries prepared with and without a dispersing agent were poured into small jars. The solids were allowed to settle out of suspension and the supernatant fluid was siphoned off. The sediments were air-dried and carefully removed from the jars. The undisturbed top surfaces of the air-dried sediments from slurries prepared with and without a dispersing agent were viewed in a scanning electron microscope and the images are shown in Figure 2. Even though the top surfaces had not been exposed to any stress, all of the platelets that settled out of the slurry prepared with a dispersing agent are clearly parallel and only the faces are visible. The platelets that settled from the slurry prepared with no dispersing agent, however, are arranged randomly and both edges and faces are visible.

Results from x-ray diffraction tests—which are routinely used to identify the mineralogy of soil samples—may also be used to identify micro-fabric. Since measured x-ray diffraction patterns represent material from the surface to a depth of 30 to 50 microns beyond the surface (Archer 1969), this technique yields results that are more representative of the sample than SEM images, which only represent the observed surface. Uncertainties related to surface preparation procedures that are necessary when natural or consolidated samples are viewed in a microscope are also alleviated. The identification of kaolin clay micro-fabric with x-ray diffraction test results was established by Sachan and Penumadu (2004) and based on the work of other researchers (Brindley and Robinson 1946; Gillot 1970; Martin and Ladd 1974; Mitchell 1956). These earlier methods either required expensive pole figure devices or the impregnation of samples with various impregnants that might disturb the existing micro-fabric. In the present study, impregnants were not used and x-ray diffraction tests were performed with a Siemens Diffraktometer (model D500), which is shown in Figure 3.

When x-rays strike a crystal in a clay particle at a certain angle of incidence, the angle of reflection is equal to the angle of incidence for Bragg's reflections. Since the angle of incidence for which this occurs is specific to the type of mineral that the x-ray is striking (Bragg's law), the angle at which x-rays are detected may be used for the identification of the mineral. Crystallographic planes in kaolin clay are divided into two categories. The first category is basal planes (001 and 002), which are parallel to the platelet faces. The second category is prism planes (020 and 110), which are not parallel to the platelet faces. Therefore, if the micro-fabric in a sample of kaolin clay is dispersed and the faces of the platelets are parallel to the surface being studied with x-ray diffraction, then the relative intensity values at angles of incidence corresponding to basal planes are increased and those corresponding to prism planes are small.

Figure 4 shows x-ray diffraction patterns from tests performed on the air-dried sediments from slurries prepared with and without a dispersing agent. These were the same sediments observed in the SEM and shown in Figure 2. Figure 5 shows x-ray diffraction patterns corresponding to samples from one-dimensionally consolidated kaolin clay specimens with flocculated and dispersed micro-fabric. The surfaces that were studied with x-ray diffraction were parallel to the direction of preferred platelet orientation (perpendicular to the axis of vertical loading in the consolidometer for the consolidated samples and gravity for the sediments). In the diffraction patterns corresponding to sediments from slurries prepared with a dispersing agent and consolidated samples with dispersed micro-fabric, the only significant peaks are those that correspond to basal planes, i.e. the faces of the platelets. Therefore, the platelets were oriented parallel to each other and the surface being examined. In the diffraction patterns corresponding to sediments from slurries prepared without a dispersing agent and consolidated samples with flocculated micro-fabric, the diffraction peaks corresponding to the basal planes (platelet faces) are present; but there are also other peaks present. These peaks correspond to the prism planes, indicating that platelets were oriented in different directions. The similarities between Figures 4a and 5a and Figures 4b and 5b indicate that the geometric arrangement of platelets (i.e. micro-fabric) was defined before axial load was applied in the slurry consolidometer. This verifies the observations made with the SEM: micro-fabric is influenced by the electro-chemical properties of the pore fluid much more significantly than it is by mechanical inter-particle forces—at least at the slurry stage. Furthermore, the presence of basal peaks at the same angles in diffraction patterns corresponding to samples with dispersed and flocculated micro-fabric indicates that the atomic structure of the platelets was not changed by the addition of sodium hexa-metaphosphate to kaolin clay slurry. Therefore, the mechanical properties of the platelets may be assumed to remain the same when slurries are prepared with a dispersing agent.

It was expected that one-dimensionally consolidated samples that were prepared with a dispersing agent would have more anisotropy of platelet arrangement than sediments from slurries prepared with a dispersing agent, due to the one-dimensional load. On observation of Figures 4b and 5b, however, the sediments from slurries prepared with a dispersing agent appear to have more anisotropy of platelet arrangement than the one-dimensionally consolidated samples with a preconsolidation stress of 207 kPa that were prepared with a dispersing agent. At the slurry stage, the platelets have more room to move into their most stable arrangement according to electro-chemical forces, without interference from adjacent platelets. When consolidated specimens with dispersed micro-fabric were prepared, the platelets did not have adequate time to settle into their most stable configuration (which took two months during the settling column testing program). Instead, they were forced to consolidate by the externally applied stress. Furthermore, on observation of Figures 4a and 5a, the sediments from slurries prepared without a dispersing agent appear to have a more random arrangement of platelets than one-dimensionally consolidated samples with flocculated micro-fabric. This is because anisotropy was induced by the one-dimensional stress applied to consolidated specimens with flocculated micro-fabric. Since the sediments from slurries prepared without a dispersing agent were only subjected to the self-weight of the solids, they had less anisotropy of platelet arrangement than the consolidated samples with flocculated micro-fabric.

4. EFFECTS OF DISPERSING AGENT ON KAOLIN CLAY SLURRY:

Measurements of pH were made in this study using an Orion temperature-correcting pH meter (model 250A). The pH of the de-aired, de-ionized water used during specimen preparation was 6.3. When sodium hexa-metaphosphate was added to create a 2% solution, the pH increased slightly to 6.5. The pH of kaolin clay slurry prepared without a dispersing agent was measured as 4.6. Since the slurry was rather viscous and it was suspected that this may interfere with the instrumentation, slurry was made with twice the water content and the pH was measured as 4.7. The pH of slurry prepared with a dispersing agent was measured as 6.1. This increase in pH corresponding to the change in micro-fabric supports the statements by Lambe (1958) and Mitchell (1993) that kaolin clay platelets have a positive charge on their edges (and, therefore, flocculated micro-fabric) in a low pH environment and that increasing pH causes dissociation of platelets. It should be noted, however, that slurry prepared with a dispersing agent was still slightly acidic.

The electric potential due to the surface charge of fine-grained materials that are surrounded by pore fluid decreases with distance from the surface of a given particle. This decrease in potential is modeled in double layer theory and is due to the oppositely charged ions that are adsorbed on the particle surfaces and contained in the diffuse double layer (Mitchell 1993). Zeta potential is the electric potential at a distance from the surface of a particle in a colloid suspension corresponding to the edge of the adsorbed ions that move with the particle under an applied electric field (the fluid shearing plane). Figure 6 conceptually shows the location of the zeta potential for a spherical particle. Zeta potential is directly related to the double layer repulsive force between two particles in a mineral suspension (Johnson et al. 2000). Kaolin clay platelets are larger than what are typically referred to as colloids, but they are sufficiently small that they remain in suspension long enough to make zeta potential measurements. In this study, the zeta potential has been measured for diluted slurries (suspensions) prepared without a dispersing agent as well as slurry prepared with a dispersing agent and diluted with a 2% solution of sodium hexa-metaphosphate. Zeta potential was determined from electrophoretic mobility using a Pen Kem Laser Zee Meter (model no. 501). Use of this device necessitates diluting the slurries such that they are nearly transparent because the microscope used to monitor the particle movement must be focused on a certain plane in the cell that is filled with the colloid suspension. This is the plane where the fluid is stationary and, therefore, the observed movement of particles is only due to the applied electric field.

The average measurement of zeta potential from 16 tests for platelets in slurry prepared without a dispersing agent was -44.4 mV with a standard deviation of 1.7 mV. The average measurement of zeta potential for platelets in slurry prepared with a dispersing agent was -48.7 mV with a standard deviation of 1.0 mV. The negative value of zeta potential verifies that the net surface charge of the platelets is negative. The slight difference in zeta potential between platelets in suspensions prepared with and without a dispersing agent is a result of the additional ions that surround and move with platelets in suspensions and slurries prepared with a dispersing agent. The fact that the change in zeta potential is slight indicates that the differences in micro-fabric between specimens prepared with and without a dispersing agent are indeed due to changes in the *variation* of the effective surface charge between that edges and faces (i.e. the effective removal of positively charged edges due to surrounding negative ions) rather than changes in the amount of net surface charge. Zeta potential only depends on the net surface charge and the electro-chemical properties of the pore fluid, so if the significant change in micro-fabric accompanying the addition of a dispersing agent was due to changes in the net surface charge, then the change in zeta potential would be more significant when a dispersing agent is present in the suspension.

The consistency of slurries prepared with and without a dispersing agent was observed to be very different and this difference was quantified with thixotropic loop rheology measurements. Viscosity of a fluid is defined as the slope of the curve when shear stress is plotted as a function of shear rate and it varies with the shear rate that is applied for non-Newtonian fluids. The viscosity of slurry prepared with and without a dispersing agent was measured as a function of shear rate using a Rheometric Scientific LS-ARES LC test station with cup and bob geometry. The test station and the cup and bob that were used are shown in Figure 7. The cup was filled with slurry and torsion was applied to the submerged bob in order to impose target shear rates. The torsional resistance to rotation was measured using a very precise air bearing based torque measuring system in order to obtain the corresponding shear stresses. Figure 8 shows the observed viscosity as a function of shear rate for slurries prepared with and without a dispersing agent. If 60 s^{-1} is arbitrarily chosen as a shear rate for comparison, then the viscosity of slurry prepared without a dispersing agent is seen to be 1.4 Pa-s while that of slurry prepared with a dispersing agent is only 0.013 Pa-s.

Plots of shear rate vs. shear stress are shown for slurries prepared with and without a dispersing agent in Figure 9. It may be observed that, for slurry prepared without a dispersing agent, the shear stress was smaller when the shear rate was initially increased to a given value than it was when the shear rate was subsequently decreased to the same value. This is called rheopectic behavior and indicates that, when the platelets were disturbed by the applied shear stress in slurry prepared without a dispersing agent, additional structure was formed. This may be explained in terms of additional bonding between the oppositely charged edges and faces of platelets. Slurry prepared with a dispersing agent, on the other hand, showed a larger shear stress during the initial increase in shear rate than that when the shear rate was subsequently decreased. This is called thixotropic behavior and indicates that, when shear stress was applied to slurry prepared with a dispersing agent, existing structure was broken down further. The thixotropic loop observed in slurry prepared with a dispersing agent was thin and the shear stresses being measured were small relative to the resolution of the measurements; but thixotropic behavior is typical for shear thinning fluids and it is therefore reasonable to assume that the observed thixotropic behavior is representative of slurry prepared with a dispersing agent.

The liquid limit of the kaolin clay that was used in this study was measured as 59. When a 2% solution of sodium hexa-metaphosphate was used instead of water, the liquid limit was reduced to 32. This is directly related to the difference in viscosity of slurries prepared with and without a dispersing agent and both of these observations are due to changes in the surface charge distribution, which cause clusters of platelets to disassociate. Table 2 summarizes the effects of the addition of sodium hexa-metaphosphate to kaolin slurry on pH, zeta potential, viscosity, and liquid limit.

5. LEECHING TESTS PERFORMED UNDER APPLIED VERTICAL STRESS:

Chen and Anandarajah (1998) showed that when kaolin clay suspensions were poured into settling columns and a dispersing agent ($AlCl_3$) was added after the height of the sediment reached equilibrium, the height of the sediment decreased significantly. These tests were referred to as "leeching tests". When the amount of dispersing agent was decreased, by removing supernatant fluid and replacing it with de-ionized water (cyclic leeching test), the height of the sediment did not increase. In that study, the kaolin clay was only under its self-weight.

During the present study, it was hypothesized that the significance of the introduction of a dispersing agent may decrease in the presence of appreciable inter-particle, mechanical forces. This hypothesis was tested in the present study by performing leeching tests under an applied vertical effective stress. Various vertical stresses were applied to consolidation test samples with flocculated micro-fabric using incremental load consolidation testing systems and primary consolidation was allowed to complete. Then, sodium hexa-metaphosphate was added to the surrounding water to create a 2% solution. The dispersing agent diffused (or leeched) into the sample and displacement was monitored with time as the micro-fabric changed until the height of the sample remained constant again. The change in void ratio associated with the measured displacement is directly related to the change in micro-fabric, and very significant displacements were observed after the dispersing agent was introduced. A test similar to the "leeching test", proposed by Chen and Anandarajah (1998), was also performed to serve as a reference point. Slurry was prepared with no dispersing agent at twice the normal initial water content, then poured into a 1000 mL graduated cylinder (settling column). After the height of the sediment stabilized, dispersing agent was added to the supernatant fluid in the settling column to create a 2% solution. The height of the sediment was then monitored with time until it again reached a state of equilibrium.

For each test that was performed, Table 3 shows the ultimate applied vertical stress, the initial void ratio of the sample (e_o), the void ratio of the sample after primary consolidation was completed under the applied vertical stress (e_l), and the final void ratio that was reached after leeching (e_f). The data given for an ultimate applied vertical stress of 0 kPa correspond to the results of the leeching test that was performed on slurry in a settling column. For this case, the initial void ratio (e_o) is the void ratio of the slurry; the void ratio after consolidation (e_l) is the void ratio of the stabilized sediment; and the final void ratio that was reached after leeching (e_f) is the final void ratio of the sediment after the dispersing agent was added to the supernatant fluid under the existing magnitude of vertical stress. The average void ratios of samples that were prepared with a dispersing agent under the same vertical effective stress (e_d) are also given in Table 3. These values were obtained from consolidation test data corresponding to samples that were prepared with a dispersing agent and correspond to the end of primary consolidation under the specific load. The "average void ratio of samples prepared with a dispersing agent under the same vertical effective stress" (e_d) corresponding to an applied vertical stress of 0 kPa in Table 3 is the average void ratio of the sediments from slurries prepared with a dispersing agent (from the settling column tests). Finally, the "degree of dispersion" is shown in Table 3 and defined below:

$$\text{Degree of Dispersion} = \frac{(e_l - e_f)}{(e_l - e_d)} \quad (1)$$

The void ratio values in Equation 1 correspond to a constant magnitude of vertical effective stress. Note that the degree of dispersion is affected by the slight variations in the initial void ratio of the samples. The degree of dispersion represents the change in micro-fabric due to the addition of a dispersing agent after vertical effective stress is applied as a fraction of the change in micro-fabric that occurs when the dispersing agent is added at the slurry stage.

The results show that none of the leeching test samples reached the void ratio of samples prepared with a dispersing agent under the same vertical effective stress, but they did consolidate significantly when the dispersing agent was added despite the fact that the vertical stress remained constant. This indicates that the electro-chemical properties of the pore fluid are more important in defining the micro-fabric at early stages of the formation of the clay. Therefore, the sensitivity of natural clays to remolding even when the pore fluid from the field is used may be explained; the pore fluid that is sampled from the field is not necessarily the same pore fluid that was present at the time of the formation of the clay. The fact that all of the samples consolidated significantly with the addition of the dispersing agent—even when high effective vertical stresses were present—indicates that the properties of the pore water fluid that is introduced when load is already being carried by the clay are more significant than previously suspected (Bennett and Hurlbut 1986; Mitchell 1993).

There are two factors that stop the void ratios of leeching test samples from reaching the level of samples prepared with a dispersing agent under the same applied vertical effective stress. First, there was no mechanical disturbance to break up bonded platelets as the high shear mixing does during the preparation of specimens with dispersed micro-fabric. Second, and probably more significantly, the mechanical contacts that presumably carry much of the effective stress through the solid soil skeleton could stop the platelets from moving into a parallel arrangement. That is to say that, due to the fact that the void ratio is much smaller than that at the slurry stage, the platelets do not have adequate room to move into their most stable position (parallel).

The samples that were exposed to higher stresses reached a lower void ratio, but the degree of dispersion was greater for samples under smaller stresses. This is because, at higher vertical effective stress, there are more mechanical contacts and they carry larger forces to resist the rearrangement of platelets. Also, the initial void ratio is smaller at high vertical effective stresses and, therefore, the platelets have less room to move. It is interesting to note that the x-ray diffraction data indicates that the sediment from slurry prepared with a dispersing agent has a more parallel arrangement of platelets than specimens with dispersed micro-fabric that have been consolidated to 207 kPa (30 psi). This can be explained if one considers the fact that platelets which settle from suspension are completely able to move and thus can arrange themselves parallel to each other more easily than those that are forced to consolidate more quickly by an externally applied state of stress.

6. CONTROLLED-RATE-OF-STRAIN CONSOLIDATION TESTING:

Controlled-Rate-of-Strain (CRS) consolidation tests yield void ratio as a function of effective stress and are therefore comparable to incremental load tests. Rather than applying a known stress and waiting for the excess pore pressure to dissipate in an incremental form, a specified strain rate is used for CRS testing and the load, displacement, cell pressure, and excess pore pressure at the base of the test sample are measured. The average effective stress is computed using a simplified theoretical solution to the applied boundary value problem (Wissa et al. 1971). Throughout the test, the excess pore pressure during the application of vertical strain is assumed to be zero at the top of the sample (where full drainage is allowed), and maximum at the impermeable base—where it is measured.

CRS consolidation tests have several advantages over traditional incremental load tests. Incremental load tests can take a very long time (several weeks) to complete depending on the permeability and compressibility of the soil being tested as well as the number of data points desired to accurately define the consolidation curve. CRS tests, on the other hand, can be completed in a relatively short duration (hours or days) even for clays with low permeability. A second advantage of CRS tests is that they are more easily computer automated than incremental load tests, which makes them less labor intensive. Because they are typically computer automated, CRS tests also provide a continuous relationship between void ratio and effective stress, whereas incremental load tests only provide one data point for each stress increment. CRS tests are carried out in a pressurized cell, which facilitates saturation of samples with back pressure. Finally, CRS test data may be used to determine permeability and coefficient of consolidation.

One of the boundary conditions in CRS theory is that consolidation is taking place at a constant rate of strain. The method suggested by ASTM D 4186-89 for determining the strain rate to be applied, however, is a trial and error approach and has no rigorous theoretical basis. The reason that CRS tests can be completed much more quickly than incremental load tests is that it is not necessary to wait for the excess pore pressure to dissipate because the excess pore pressure is continuously measured at the base of the sample. According to CRS theory, the excess pore pressure is parabolically distributed with a maximum value at the base to zero at the top of the deforming sample (Wissa et al. 1971). The pore pressure ratio is defined as the ratio of the excess pore pressure at the base of the test sample to the total applied vertical stress. ASTM suggests that the pore pressure ratio be maintained between 0.03 and 0.30 throughout the test. Therefore, a strain rate must be selected that will not violate this restriction. The reason for the restriction is that if the strain rate (and correspondingly the pore pressure ratio) is too high, then the difference between the void ratio and effective stress at the top and bottom of the sample will be too great causing errors in the interpretation of data; assumptions of constant permeability and linear distribution of void ratio will be violated. If the strain rate is too low, then excess pore pressure will not develop and there will be no basis for computing permeability or coefficient of consolidation (Lee et al. 1993; Terzaghi et al. 1996). While most research has supported this restriction, there has been some work that suggests that the restriction may be unnecessary—particularly for non-structured clays (Sheahan and Watters 1996, 1997). The work that supports the restriction of pore pressure ratio has disagreement as to what an acceptable range is and the suggested maximum values range from 0.05 to 0.50 (Gorman et al. 1978; Mesri and Feng 1992;

Sällfors 1975; Smith and Wahls 1969; and Wissa et al. 1971). These disagreements seem to depend on the particular type of clay being tested and are typically based on comparisons to incremental load test results.

Lee (1981) developed a finite strain solution for CRS consolidation, which—unlike the small strain theory—showed that consolidation was affected by a dimensionless strain rate. Numerical studies showed that significant changes in the solution appeared when the dimensionless strain rate was greater that 0.1 and this was proposed as a more logical criterion for determining the proper strain rate. Lee et al. (1993) subsequently implied that this typically corresponds to a pore pressure ratio of approximately 0.15. Due to the low permeability of samples with dispersed micro-fabric, the suggested maximum value of pore pressure ratio suggested in ASTM D 4186 was slightly exceeded for samples with dispersed micro-fabric in the present study even when the load frame was set at the lowest possible screw speed. This should not be a reason for concern, however, because the suggested maximum value for pore pressure ratio was only exceeded briefly in the initial recompression zone at the starting phase of the CRS consolidation tests on samples with dispersed micro-fabric. The data from the initial recompression stage were not used in the data interpretation for the present study; the swelling index (*Cs*) was obtained from the unloading portion of the test data. Furthermore, the results from all CRS tests were verified with incremental load tests. It is of interest to note that Smith and Wahls (1969) showed agreement between incremental load tests and CRS tests at different strain rates for kaolin clay with pore pressure ratios ranging up to 0.50. The small strain theory of Wissa et al. (1971) was used for data interpretation in this study, as recommended by the current ASTM standard.

For typical consolidation problems, the assumption of small strain does not cause significant problems (Mesri and Rokhsar 1974).

In past studies there has been little analysis of CRS testing during the unloading stage. It is useful to study this aspect of CRS testing because consolidation properties obtained during unloading represent consolidation behavior in the over-consolidated region. There are some issues that must to be resolved for suitable analysis of data obtained during unloading in CRS tests. During the unloading stage of CRS testing, negative excess pore pressure is typically developed because the solid skeleton rebounds, which causes an increase in the total volume of the sample. The corresponding decrease in excess pore pressure causes water to flow back into the sample from the top (since the base is impermeable). Since this takes time, due to the low permeability of clay, the excess pore pressure decreases (typically becoming more negative) throughout the unloading phase of the test. If the test is stopped before unloading (and held at a constant deformation) until the positive excess pore pressure dissipates, then the stress will decrease due to relaxation and pore pressure dissipation and there will be a discontinuity in the consolidation curve. If unloading is started immediately, however, then there will be a positive excess pore pressure present when unloading begins and a transient error in data interpretation will occur as the positive excess pore pressure decreases due to the fact that CRS theory assumes a constant rate of strain is maintained throughout the test. A similar transient error occurs at the start of CRS tests, but at this stage the excess pore pressure starts at zero and goes positive. When the conditions stabilize, the data may be interpreted according to the same theory that is used during the initial loading, but the effective stress will be greater than the total stress because the average excess pore pressure is negative.

One idea that was proposed by Wissa et al. (1971) to solve this problem is to maintain a constant load (rather than constant deformation) until primary consolidation is complete (i.e., until excess pore pressure has dissipated), and then begin the unloading portion of the test. This solution will also cause a discontinuity in the consolidation curve, but the rebound curve will still span the entire range of stress desired and the unloading may be thought of as a separate test. One advantage of holding a constant load before unloading is that if deformation were measured during this time some insight into the significance of secondary consolidation could be gained. Since CRS testing is deformation controlled, however, this solution requires feedback control and the equipment in this study did not have the capability to do this. Mesri et al. (1994) describes a method to use a deformation controlled setup to measure swelling by quickly unloading to zero load and allowing the sample to swell to a specified void ratio, and monitoring the load. Since the swelling pressure goes beyond the end-of-primary swelling curve, this method can be used in conjunction incremental unloading data to study secondary swelling—which is not the objective of this study. In this study, unloading was started immediately after loading in order to obtain a continuous consolidation curve. In an attempt to avoid the associated transient error in data interpretation, the data points at the start of the unloading curve were not used in computing the swelling index values.

7. CONSOLIDATION TESTING PROGRAM AND DATA ANALYSIS:

Controlled-rate-of-strain (CRS) and incremental load (IL) consolidation tests were performed on samples with flocculated and dispersed micro-fabric in the vertical and horizontal directions. The vertical direction is the direction in which axial load was applied in the slurry consolidometer during specimen preparation; and the horizontal direction is perpendicular to the vertical direction (see Figure 10). Samples on which load was applied in the vertical direction (i.e. the same direction in which load was applied in the consolidometer) during CRS and IL consolidation testing are referred to as vertical samples and those on which load was applied in the horizontal direction are referred to as horizontal samples. CRS and IL tests were performed according to ASTM D 4186-89 and D 2435-96, respectively.

The CRS tests were performed in a custom-built test cell that was placed in a Geotest S5770 deformation controlled compression machine. The disassembled cell and the entire CRS testing apparatus are shown in Figure 11. The standard consolidation ring containing the test sample (which was also used for the incremental load consolidation tests) was placed against an o-ring that fit in a groove in the impermeable base. A piece of porous plastic separated the sample from a channel that led to a pressure transducer that was used to measure the excess pore pressure at the base of the samples. A valve allowed back pressure to be applied simultaneously to the bottom of the submerged sample and the surface of the water in the cell. The back pressure was measured throughout the test with a second pressure transducer. The applied load was measured using a load cell and the amount of deformation was measured with an LVDT. All measurements were made continuously through the test with a data acquisition system.

The load was transmitted to the sample with an aluminum rod; and o-rings sealed the top and bottom of the cell as well as the opening where the loading rod entered the cell. The incremental load tests were completed using a Wykeham Farrance incremental load apparatus (model no. 24001) with a lever arm to apply axial load.

Mesri and Feng (1992) showed that if a strain rate is chosen that causes near-zero excess pore pressure (and thus pore pressure ratio), then the void ratio-log of effective stress curve will be practically the same as that from the end-of-primary (EOP) consolidation data obtained in an incremental load test. The EOP consolidation curve was shown to be representative of behavior in the field regardless of the layer or sample thickness by Mesri and Choi (1985). If excess pore pressure is developed, however, then there will be a shift between the consolidation curve obtained from the CRS test and that obtained from the incremental load test. The two curves will be parallel, however, so the slopes are still directly comparable (Terzaghi et al. 1996). In the present study, a number of tests were repeated for each micro-fabric and direction of axial loading until an acceptable standard deviation was obtained. The results for each micro-fabric and direction of axial loading were verified with at least one incremental load test.

For each direction and micro-fabric, the target strain rate was chosen based on the pore pressure ratio, as suggested by the ASTM standard for CRS testing (ASTM D4186-89). For samples with both flocculated and dispersed micro-fabric the unloading strain rate was found to yield appropriate pore pressure ratios when it was half of the magnitude of the strain rate used during loading. The average strain rates applied for samples with flocculated and dispersed micro-fabric were 0.10 and 0.02 % per minute, respectively.

In each CRS test, a maximum effective stress of 1000 kPa was reached, and then the effective stress was decreased to a value less than 200 kPa. The effective stress was then increased to a value greater than 1000 kPa. These effective stress values were chosen to yield sufficient data to obtain the virgin compression index and swelling index. The virgin compression index (*Cc*) for each test was determined from a best-fit line through the data points between effective stress values of 400 kPa and 1000 kPa in the normally consolidated zone. This range of vertical effective stress values corresponded to the zone that appeared to be linear on a semi-log scale. The swelling index (*Cs*) was determined from a best-fit line through the data points on the unloading curve between 900 kPa and 200 kPa. These values were chosen to avoid the transient error associated with the beginning of the unloading phase of CRS testing.

8. CONSOLIDATION TEST RESULTS:

Table 4 shows the values of virgin compression index (*Cc*), swelling index (*Cs*), and initial void ratio for all of the consolidation tests performed in this study. Figure 12 shows representative CRS consolidation curves (void ratio vs. log of effective stress) for vertical and horizontal samples with flocculated and dispersed micro-fabric. Figure 13 shows a comparison between the consolidation curves obtained from CRS tests and IL tests on vertical and horizontal samples with flocculated and dispersed micro-fabric. For clarity of comparison, the difference between the initial void ratio and the void ratio at each effective stress was taken to normalize the results. Samples with flocculated micro-fabric are observed to have a significantly higher virgin compression index than samples with dispersed micro-fabric. This observation holds in both the vertical and horizontal directions. As for the over-consolidated zone (unloading portion of consolidation tests), the swelling index appears to depend more on the direction of one-dimensional consolidation than micro-fabric. That is to say, the values of the swelling index for a given direction of axial loading and micro-fabric are closer to those corresponding to samples with different micro-fabric when axial load was applied in the same direction than they are to those with the same micro-fabric when axial load was applied in perpendicular directions. In fact, there is no statistically significant difference between the average swelling indexes for samples with flocculated and dispersed micro-fabric in either the vertical or horizontal directions of loading (average values of *Cs* for flocculated micro-fabric are within the range of that for dispersed micro-fabric plus or minus one standard deviation—and vice versa). This implies that the swelling index is independent of micro-fabric for the kaolin clay used in this study.

Inelastic (non-recoverable) deformations are those resisted by inter-particle friction (Terzaghi et al. 1996) and elastic (recoverable) deformations are those resisted by a combination of straining of the particles (mostly bending for clay platelets), double layer repulsive forces, and—for swelling clays in the presence of excess water—the attraction between water and the surfaces of platelets and adsorbed ions. Mesri et al. (1994) showed that for some fine grained materials the attraction of water to particle surfaces causes the most significant portion of swelling by allowing clay shale to rebound without access to water, then adding water and monitoring deformation. The bonding between successive layers in kaolinite, however, is strong enough to prevent inter-layer swelling (Mitchell 1993). It is reasonable to hypothesize that bending is less significant in samples with dispersed micro-fabric (because the platelets are parallel), but that double layer repulsion is more significant (because the platelets are more closely spaced) and that these differences—perhaps coincidentally—served to cancel each other out. There are positively charged sodium ions present in specimens prepared with a dispersing agent that are not present in specimens prepared without a dispersing agent and these ions would tend to be adsorbed on or contained in the diffuse double layers of the negatively charged platelet faces. This would decrease the repulsive forces between the platelets. Also, water molecules would possibly be less attracted to the platelet faces in samples with dispersed micro-fabric than they are in samples with flocculated micro-fabric. This may also (in addition to more platelet bending) offset the presumed greater potential for double layer repulsive forces that are present in samples with dispersed micro-fabric, causing them to have swelling indexes similar to samples with flocculated micro-fabric.

For samples with both flocculated and dispersed micro-fabric, the virgin compression index and the swelling index are seen to be greater in the vertical direction than they are in the horizontal direction. Degree of anisotropy, elastic degree of anisotropy, and plastic degree of anisotropy (of one-dimensional consolidation behavior) are respectively defined as:

$$\text{Degree of Anisotropy} = \frac{(Ccv - Cch)}{Ccv} \qquad (2)$$

$$\text{Elastic Degree of Anisotropy} = \frac{(Csv - Csh)}{Csv} \qquad (3)$$

$$\text{Plastic Degree of Anisotropy} = \frac{(Ccv - Csv) - (Cch - Csh)}{(Ccv - Csv)} \qquad (4)$$

The v and h subscripts in the equations 2, 3, and 4 respectively indicate the vertical and horizontal directions of axial loading during one-dimensional consolidation testing (samples were consolidated vertically in the consolidometer). For example, *Ccv*, is the virgin compression index obtained from a vertical sample. The degree of anisotropy and elastic degree of anisotropy may be conceptually described as the percent change from the vertical to the horizontal direction for the virgin compression index and swelling index, respectively. The difference between the virgin compression index and the swelling index is related to the amount of plastic deformation that occurs during one-dimensional consolidation. Therefore, the plastic degree of anisotropy is the percent change in the amount of plastic deformation between samples on which load was applied in the vertical and horizontal directions. A degree of anisotropy equal to zero indicates completely isotropic one-dimensional consolidation behavior.

The average values for degree of anisotropy, elastic degree of anisotropy, and plastic degree of anisotropy are shown for samples with flocculated and dispersed micro-fabric in Table 5. It was expected that samples with dispersed micro-fabric would exhibit more anisotropy of one-dimensional consolidation properties than samples with flocculated micro-fabric because the platelet arrangement is anisotropic, but the anisotropy of both the virgin compression index (degree of anisotropy) and the swelling index (elastic degree of anisotropy) are greater for samples with flocculated micro-fabric than they are for samples with dispersed micro-fabric. The author suggests that this is because consolidation of samples with dispersed micro-fabric is controlled more significantly by double layer repulsive forces than the consolidation of samples with flocculated micro-fabric, as discussed above.

Consider an extreme case in which *all* consolidation is resisted by double layer repulsive forces between parallel platelets. The change in inter-platelet spacing would only depend on changes in volume and the resistance to consolidation would be independent of the direction of axial loading. If platelet bending is assumed to be more significant in samples with flocculated micro-fabric than in samples with dispersed micro-fabric and double layer repulsive forces are less significant, then it is logical to conclude that anisotropy in the elastic zone would be greater for samples with flocculated micro-fabric. Mesri et al. (1978) has shown that the swelling index increases with over-consolidation ratio (OCR) and, therefore, decreases with increasing effective stress. This means that the swelling index decreases with decreasing void ratio, which may be a manifestation of the decreasing significance of platelet bending as platelets move into a more parallel arrangement.

For samples with both flocculated and dispersed micro-fabric, the elastic degree of anisotropy is significantly greater than the degree of anisotropy (of the virgin compression index). For samples with both flocculated and dispersed micro-fabric, the difference between the average virgin compression index and the average swelling index (which is related to the amount of plastic deformation) is essentially the same for vertical and horizontal samples—which is the reason the plastic degrees of anisotropy are small. This indicates that anisotropy in the normally consolidated zone is only due to the anisotropy of the elastic portion of deformation and, therefore, the plastic portion of the consolidation behavior is isotropic. The negative value for plastic degree of anisotropy for samples with dispersed micro-fabric indicates that, in samples with dispersed micro-fabric, there is more plastic deformation when load is applied in the horizontal direction than there is when load in applied in the vertical direction while. This can be explained because when the platelets are parallel to each other and load is applied in the same direction as the preferred alignment, the platelets would tend to slide into a more closely spaced arrangement (and the sliding would be resisted by friction). The values of plastic degree of anisotropy are not very reliable because the differences between the virgin compression index and the swelling index are small compared to the associated standard deviations. The plastic degree of anisotropy should perhaps be interpreted as approximately zero for both flocculated and dispersed micro-fabric (indicating isotropic plastic consolidation behavior).

The value of the virgin compression index is much closer to the value of the swelling index for samples with dispersed micro-fabric than it is for samples with flocculated micro-fabric. This implies that there is more plastic deformation involved when samples with flocculated micro-fabric undergo consolidation. In order to quantify this difference as well as changes in the amount of plasticity with the direction of axial loading, degree of plasticity (of one-dimensional consolidation behavior) for a given micro-fabric and direction of axial loading is defined as:

$$\text{Degree of Plasticity} = \frac{(Cc - Cs)}{Cc} \qquad (5)$$

Degree of plasticity may be conceptually explained as the percent change between the virgin compression index and the swelling index. Therefore, a degree of plasticity of zero would indicate completely elastic consolidation behavior. Table 6 contains the average degrees of plasticity for vertical and horizontal samples with flocculated and dispersed micro-fabric. The degree of plasticity is significantly greater for samples with flocculated micro-fabric than it is for samples with dispersed micro-fabric for both vertical and horizontal loading. The greater degree of plasticity corresponding to samples with flocculated micro-fabric is due to the fact that, in samples with dispersed micro-fabric, essentially all platelet re-orientation is completed in the consolidometer at much lower vertical stresses (at the slurry stage). Particle re-orientation is associated with plastic (non-recoverable) deformations because, if a particle moves relative to adjacent particles as a result of an increase in vertical effective stress and the movement was resisted by friction, then when the stress is removed, the particle will not move back to its original position. If the particle movement was resisted by elastic strain, double layer repulsive forces, or possibly the attraction of water to the platelet surface (for swelling clays), on the other hand, then the particle will move back to its original position when the stress is removed. The degrees of plasticity corresponding to samples with both flocculated and dispersed micro-fabric are also greater for horizontal samples than they are for vertical samples. This appears reasonable if it is assumed that plastic deformations are resisted by friction because, in vertical samples—which have a preferred orientation that is perpendicular to the axis of loading—platelets would tend to bend or rotate to a position perpendicular to the axis of loading. Horizontal samples—which have a preferred orientation that is parallel to the axis of loading—would tend to slide into a more tightly packed arrangement. The higher degree of plasticity in horizontal samples provides support for the authenticity of the negative value for degree of plastic anisotropy that was calculated for dispersed micro-fabric.

Another observation that can be made is that the consolidation curves corresponding to vertical and horizontal samples with dispersed micro-fabric have a less abrupt transition between the over-consolidated and normally consolidated zones than those with flocculated micro-fabric. That is to say, the preconsolidation stress is less apparent and the plot looks more like a single curve. The observation that preconsolidation stress is not as well defined in consolidation curves corresponding to samples with dispersed micro-fabric is partly a manifestation of the fact that the degree of plasticity is lower (and therefore that *Cc* is closer to *Cs*), but the transition between the over-consolidated zone and the normally consolidated zone also takes place over a greater range of effective stresses. Terzaghi et al. (1996) explains that when clays have significant bonding (interpreted here as a result of oppositely charged faces and edges) and cementation, the transition to the normally consolidated zone is more abrupt. Therefore, it is logical that consolidation curves corresponding to samples with flocculated micro-fabric would have a more abrupt transition between the over-consolidated and normally consolidated zones than those corresponding to samples with dispersed micro-fabric.

9. SUMMARY AND CONCLUSIONS:

Reconstituted kaolin clay specimens with two types of micro-fabric have been made from the same powdered kaolin clay. Variations in micro-fabric were achieved by the introduction of a dispersing agent (sodium hexa-metaphosphate) at the slurry stage. Kaolin clay specimens (with no dispersing agent added) have flocculated micro-fabric, which means that the edges of platelets are attracted to the faces of other platelets and agglomerations of platelets with essentially random orientation result. When a dispersing agent is added to the slurry, these agglomerations are broken up and the platelets arrange themselves parallel to each other according to the electro-chemical forces that are present. The preferred direction of platelet orientation is perpendicular to the direction of maximum load (e.g. the direction of axial load in the consolidometer or the direction of gravity). It has been shown that the micro-fabric is determined by the electro-chemical properties of the pore fluid even in the absence of mechanical forces by allowing the solids to settle from slurry in graduated cylinders and observing the final height of the resulting sediment.

The change in micro-fabric associated with the addition of a dispersing agent to the slurry has been observed with scanning electron microscope (SEM) images and x-ray diffraction data. These techniques have been used to study both the sediments from slurries that were poured into small jars and one-dimensionally consolidated samples with a preconsolidation stress of 207 kPa (30 psi). The change in micro-fabric has been quantified in terms of the void ratio of sediments of slurries prepared with and without a dispersing agent. The effects of the dispersing agent on kaolin clay slurry have been studied. The zeta potential of the clay platelets in suspension changed slightly as a result of the addition of the dispersing agent, indicating a slight change in the net surface charge of the particles. The pH and viscosity of the slurry also change with the addition of a dispersing agent. The differences in compressibility between samples with flocculated and dispersed micro-fabric that have been observed in this study may have been slightly affected by factors other than the micro-fabric, such as additional ions that cause changes in the measured zeta potential of the platelets and the pH of the bulk samples, but these changes are more accurately described as the *causes* of the change in micro-fabric.

"Leeching tests" were performed in settling columns and incremental load consolidation test setups in which the dispersing agent was added after the micro-fabric was already formed and various vertical effective stresses were already present. It has been concluded from these tests that clay micro-fabric is determined by both the electro-chemical properties of the platelets and the pore fluid at the slurry or suspension stage and—to a lesser, but still very significant degree—the electro-chemical properties of the pore fluid that is currently present. This is shown by the dramatic changes in void ratio under a constant effective stress that occur when a dispersing agent is added to the pore water, even when significant vertical effective stresses are being carried by the solid skeleton. Specifically, if the edges and faces of platelets are oppositely charged and the edges are not surrounded by oppositely charged ions (such as those resulting from the addition of a dispersing agent), then flocculated micro-fabric will be formed. If the effective surface charge is of the same sign on the edges and faces—be it due to the addition of a dispersing agent or naturally—then dispersed micro-fabric will form and the preferred direction of orientation will be perpendicular to the direction of the maximum stress.

It has been shown that the change in zeta potential of platelets in suspension is small when suspensions are prepared with and without a dispersing agent, from which it is concluded that the change in micro-fabric is due to the removal of *variation* of surface charge. Mesri and Olsen (1971) recognized surface charge distribution as a physio-chemical variable affecting micro-fabric, but this study has demonstrated its importance even in the presence of high, mechanical, inter-particle contact forces (with leeching tests performed under an applied vertical effective stress). Changes in the electro-chemical properties of the pore water fluid can change the micro-fabric by removing surface charge variation between platelet edges and faces even if bonds are already formed between edges and faces and the bonds carry significant mechanical forces. This may not be the case for soils with significant cementation—especially in the over-consolidated zone. These findings serve as an explanation of the significant effect that reconstituting clay from the field can have on its behavior even when the pore fluid from the field is used. When sensitive clay is reconstituted, structure could be destroyed that was formed according to the electro-chemical properties of the pore fluid that was present at the time when the structure was formed. The pore fluid that is present at the time of sampling does not necessarily have the same properties as that which was present when the present structure of the clay was initially formed and, therefore, when the clay is reconstituted, different structure may be formed.

Controlled-rate-of-strain (CRS) and incremental load (IL) consolidation tests have been performed on samples with both flocculated and dispersed micro-fabric. During these consolidation tests, load was applied in both the vertical direction (perpendicular to the preferred direction of platelet orientation) and the horizontal direction. The data in this study indicate that changes in micro-fabric do not significantly affect the compressibility in the over-consolidated zone for kaolin clay. This has been interpreted as at least partially coincidental. The portion of elastic consolidation that is resisted by platelet bending is believed to be greater in samples with flocculated micro-fabric and the portion resisted by double layer repulsive forces is believed to be greater in samples with dispersed micro-fabric. The decrease in the swelling index that typically accompanies increasing vertical effective stress (and, thus, decreasing void ratio) has been noted as evidence that platelet bending becomes less significant as platelets are arranged perpendicular to the axis of loading. These concepts imply that the importance of the double layer repulsive force is great—especially in dispersed micro-fabric. This also serves as an explanation of why samples with dispersed micro-fabric, which have anisotropy of platelet arrangement, exhibited greater isotropy of one-dimensional consolidation properties.

Another conclusion to be drawn from this study is that, even in highly dispersed clays with a clear preferred orientation angle plastic deformations in the normally consolidated zone during one-dimensional consolidation are independent of the direction of axial loading. The swelling index, however, is more affected by the direction of axial loading relative to the preferred platelet orientation than the amount of preference (i.e., the micro-fabric). This can be logically explained because platelets in vertical samples are more likely to bend where platelets in horizontal samples are more likely to slide into new positions. While the difference is only significant in the over-consolidated zone, both the virgin compression index and the swelling index are observed to be higher when axial load is applied in the vertical direction than the horizontal direction for samples with both flocculated and dispersed micro-fabric. The difference in the normally consolidated zone is thought to be only due to the elastic portion.

It can be concluded from this study that clays with dispersed micro-fabric exhibit less plasticity than clays with flocculated micro-fabric. In clays with dispersed micro-fabric, all locations on a given platelet repel all locations on adjacent platelets. In clays with flocculated micro-fabric, on the other hand, the edges of a given platelet are attracted to the faces of other platelets. Therefore, it is reasonable to assume that there are fewer mechanical contacts between platelets in clays with dispersed micro-fabric. If there are fewer mechanical contacts, then there will be less friction loss and, therefore, less plasticity. The rearrangement of platelets that is resisted by friction is typically dominated by the rotational movement of platelets towards a plane that is perpendicular to the axis of loading. Thus, it is intuitive that clays with dispersed micro-fabric should be less plastic. If the platelets are already arranged with a preferred orientation, then they would not rearrange as much because there is not a more tightly packed arrangement for the platelets to approach. Instead, the parallel plates would move closer together. Double layer repulsive forces provide most of the resistance to consolidation in clays with dispersed micro-fabric.

PART TWO:

RECOMMENDATIONS FOR MODELING

1. RECOMMENDATIONS FOR QUANTIFYING MICRO-FABRIC:

There are many variables to be considered when modeling one-dimensional consolidation. It has been shown in the present study that changes in micro-fabric cause significant changes in one-dimensional consolidation behavior. If a one-dimensional consolidation model were to be developed from theory, then it would be necessary to consider the geometric arrangement of platelets (i.e. micro-fabric). Stress-induced changes in micro-fabric that occur during one-dimensional consolidation at large strains could also be considered in large strain constitutive models. These stress induced changes in micro-fabric might be related to the decrease of the virgin compression index that is observed at high vertical effective stress. The void ratios of sediments from slurry obtained from settling columns tests in this study indicate that the virgin compression index is also greater at the slurry stage and, therefore, continually decreases as consolidation occurs. In order for micro-fabric to be considered in a consolidation model, it must be quantified. It is recommended that micro-fabric be quantified in terms of the average angle of platelet orientation relative to a plane parallel to the direction of preferred platelet orientation. This plane is assumed to be perpendicular to the direction in which one-dimensional load is (and has been) applied, which is typically the vertical direction. Therefore, the average orientation angle will typically be measured relative to the horizontal plane. This will be the context in which average orientation angle will be discussed for the remainder of this paper. Theoretically, the initial average orientation angle would be obtained by measuring the angle of each platelet relative to the reference plane and taking the average. Practically, the average orientation angle may be assumed, approximated from SEM images, or determined from particle orientation histograms.

These polar histograms may be obtained from SEM images according to the recommendations of Penumadu (1996).

It has been observed that, when micro-fabric changes from flocculated to dispersed, with a given type of clay, there is a corresponding decrease in void ratio. Therefore, relationship between the average orientation angle (θ) and void ratio (e) has been developed based on a simplified, two-dimensional geometric model and some assumptions. The model is similar to a phase diagram, which is a one-dimensional model, but the fact that it is two-dimensional allows another variable (average orientation angle) to be considered. Figure 14 shows the geometric model for an initial average orientation angle (θ_o) of 45 degrees. This corresponds to the theoretical limiting case for flocculated or "random" micro-fabric. If an initial average orientation angle greater than 45 degrees is obtained, then the preferred direction of platelet orientation is necessarily different from the one assumed.

In Figure 14, the rectangle containing two "platelets" represents a large volume of the clay being modeled. The length of the "platelets" in the geometric model is set to unity for ease of calculations and may be thought of as the average length of arbitrary cross sections of the platelets. The thickness of the "platelets" is defined as "effective thickness" (t_e) and is equal to the average aspect ratio of arbitrary cross sections of the platelets. Effective thickness may be calculated from a known average orientation angle and void ratio.

Effective thickness is assumed to remain constant during one-dimensional consolidation whether the consolidation is due to the application of additional one-dimensional stress or the addition of a dispersing agent under a constant state of stress.

The area of the rectangle (times a unit depth) represents the total volume of the clay (V_t); the area of the two "platelets" (2*t_e) represents the volume of solids (V_s); and the difference between the total volume and the volume of solids is the volume of voids (V_v). Since it is assumed that the clay being modeled is saturated, the volume of voids is equal to the volume of water. The dimensions of the rectangle are calculated from the geometry of the model and the initial average orientation angle according to the following equations:

$$height = \sin\theta_o \tag{5}$$

$$width = 2 * \cos\theta_o \tag{6}$$

There is a slight error associated with the ends of the platelets in the model, but this is not a concern due to the approximate nature of the model. Effective thickness is calculated from the geometry of the model, the initial average orientation angle (θ_o), and the initial void ratio (e_o) according to the following equation:

$$t_e = \frac{[\sin(\theta_o)]*[\cos(\theta_o)]}{(1+e_o)} \tag{7}$$

It is assumed that the *macro-fabric* is uniform. That is to say, arbitrary volumes of the clay containing a small number of particles have the same micro-fabric. It is also assumed that changes in the average orientation angle only depend on changes in void ratio and that all loads are applied in the vertical direction. Changes in void ratio (and the average orientation angle) may be due to an increase in one-dimensional load or the addition of a dispersing agent in the presence of vertical load (even if it is only the platelets' self-weight). The platelets in the clay are assumed to be rigid and incompressible. The change in void ratio under one-dimensional load is represented in the geometric model by keeping the width of the rectangle constant and decreasing its height. The “platelets” are forced to remain inside the rectangle by rotating towards the preferred plane of platelet orientation (the horizontal plane in the geometric model). Therefore, the volume of solids (V_s) in the geometric model remains constant during “one-dimensional consolidation” and the change in volume (ΔV) corresponding to the “displacement” is only due to a decrease in the volume of voids (V_v). The geometric model is shown before and after “one-dimensional consolidation” in Figure 14. The “displacement” (i.e. the change in the height of the rectangle corresponding to a given change in void ratio) is directly related to the change in the angle of the “platelets” that is required to keep them contained in the rectangle—which represents the total volume of the clay that is being modeled. Therefore, the new void ratio (e) may be related to the new average orientation angle (θ) by the following equation:

$$e = \left[\frac{(\sin\theta_o)(\cos\theta_o) - t_e}{t_e}\right] - \left[\frac{(\sin\theta_o - \sin\theta)(\cos\theta_o) - t_e}{t_e}\right] \qquad (8)$$

In this equation, the initial average orientation angle (θ_o) and the effective thickness (t_e) are constants. Equation 8 was derived from the following equation, which is used to calculate void ratio from displacement and initial void ratio in consolidation testing:

$$e = e_o - \frac{\Delta V}{V_s} = \frac{V_{vo}}{V_s} - \frac{\Delta V}{V_s} \qquad (9)$$

From symmetry, half of the geometric model may be considered (note that, when the height is decreased, the area of the left “platelet” that leaves the left half is the same as the area of the right "platelet" that enters the left half). For half of the geometric model:

$$V_s = t_e \tag{10}$$

$$V_{vo} = [\sin(\theta_o)]*[\cos(\theta_o)] - t_e \tag{11}$$

$$\Delta V = [\sin(\theta_o) - \sin(\theta)]*[\cos(\theta_o)] \tag{12}$$

Equations 10, 11, and 12 are substituted into Equation 9 to obtain Equation 8. Equation 8 may be rearranged to calculate the new average orientation angle (θ) from the initial average orientation angle (θ_o), the effective thickness (t_e), and the new void ratio (e). The resulting equation is:

$$\theta = \sin^{-1}\left[\sin\theta_o - \left(\frac{t_e}{\cos\theta_o}\right)\left(\frac{(\sin\theta_o)(\cos\theta_o) - t_e}{t_e} - e\right)\right] \tag{13}$$

The relationship between void ratio and average platelet orientation angle according to this equation may be approximated as linear. The average orientation angle of platelets in sediment from slurry prepared without a dispersing agent was assumed to be 45 degrees; and the change in average orientation angle was calculated with decreasing void ratio according to equation 13. The results appeared linear and an r^2 value of 0.998 was obtained. The results were reasonable when compared to SEM images taken at known void ratios.

2. RECOMMENDATIONS FOR MODELING ONE-DIMENSIONAL CONSOLIDATION:

It is widely understood that electro-chemical forces between particles significantly affect the behavior of fine grained materials. The most significant of these forces is the electrical double layer force (Mitchell 1993). Verwey and Overbeek (1948) evaluated double layer repulsive forces as a function of separation distance for flat, parallel platelets using the Gouy-Chapman theory of electrical double layer and the assumption of symmetric ions. A system of parallel platelets, however, has proven insufficient to represent clay behavior. Anandarajah and Chen (1994) used a finite difference method to evaluate the double layer repulsive force between two non-parallel platelets with various separation distances, angles of inclination between the platelets, platelet lengths, and surface charge characteristics. A monovalent system was considered in which the ions were assumed to be point charges. A simplified method developed by Derjaguin (1934), in which non-parallel platelets were replaced by a series of parallel platelets, was also used by Anandarajah and Chen (1994) to evaluate the double layer forces. The simplified method was found to yield similar results to the finite difference method.

Anandarajah (1994) employed a discrete element method to simulate the one-dimensional consolidation of illitic clay by defining a two-dimensional arrangement of identical platelets contained within a rectangle with a random number generator. The model corresponded to a specific void ratio for the assumed platelet size. The platelets were then allowed to rearrange themselves according to the double layer repulsive forces until stability was achieved. All electro-chemical attractive forces were ignored. One-dimensional consolidation was simulated by moving the top boundary of the rectangle down vertically while the side and bottom boundaries stayed in the same place and the platelets were forced to remain inside the rectangle. Friction between the walls and the platelets was neglected. As consolidation occurred, inter-particle contacts developed and were modeled as spring forces. This is routinely done in numerical modeling of granular materials and the linear spring represents the Born repulsion force—which prevents the overlapping of electron clouds. Bending of the platelets was also considered. During the simulation of consolidation, a void ratio was imposed by decreasing the total volume as described above and allowing the platelets to rearrange themselves according to the inter-particle forces and the platelet bending effect. The corresponding effective stress was determined by dividing the sum of the forces on the top and bottom boundaries by their areas.

Anandarajah and Chen (1997) developed a method for calculating the van der Waals attractive force between two clay platelets. The classical London, Hamaker, De Boer, and Lifshitz theories were combined to obtain a closed form solution for the van der Waals attractive force between two platelets. The effects of geometrical parameters such as platelet length, separation distance, and the angle of inclination between the platelets were also explored. Anadarajah (2000) included the van der Waals attractive force in a numerical simulation of kaolin clay. That study also considered grain size distribution by including platelets with multiple lengths. The lengths used were based on hydrometer analysis performed on the kaolin clay that was being simulated. Comparisons with experimental data for the kaolin clay were made in that study with some success. Yao and Anandarajah (2003) extended the discrete element model of

Anandarajah (2000) to a three-dimensional simulation that considered the double layer repulsive forces, inter-particle contacts, and the van der Waals attractive forces between platelets, but neglected platelet bending. The platelets were represented by rectangular cuboids. An informative plot of inter-platelet force as a function of separation distance for parallel platelets was also presented. This plot was constructed by considering the double layer repulsive force, van der Waals attractive force, and spring contact force at very small and negative separation distances. The theories used to calculate the electro-chemical forces become unrealistic at very small separation distances; therefore, the double layer repulsive force and van der Waals attractive force were assumed to remain constant when the separation distance became very small and the mechanical contact force was assumed to take effect. Anandarajah (2000) presented similar plots for various inclinations of non-parallel platelets.

The results of these studies may be used to take steps toward developing a model for clay consolidation based on theory rather than assuming a linear relationship between void ratio and effective stress on a semi-log scale. It is logical to attempt to model the over-consolidated zone first, so that inter-particle friction may be neglected. The significant remaining forces that resist consolidation are: platelet bending, double layer repulsive forces, van der Waals attractive forces, and contact forces. It would probably be reasonable to assume that the total effect of platelet bending and contact forces on void ratio would be linear with respect to the applied vertical effective stress. In the numerical studies described above, double layer repulsive forces were quantified by choosing system parameters to mimic a given situation as closely as possible. For example, Yao and Anandarajah (2003) modeled a system of water, kaolinite, and sodium chloride (NaCl). Parameters such as surface charge (for double layer force), Hamaker constant (for van der Waals force), size and shape of platelets, as well as dielectric constant, ion valence, and ion concentration of the electrolyte solution were chosen based on the best measurements of these parameters available. Some of them, such as platelet thickness, friction angle, normal contact spring stiffness, and shear contact spring stiffness (and cutoff) were apparently varied to achieve the best agreement with experimental data. In order to obtain a closed form equation for one-dimensional elastic consolidation (i.e. consolidation in the over-consolidated zone), all of these parameters could be lumped into coefficients that would be obtained by a regression analysis of test data. The necessary assumptions could be similar to those made in the discrete element models discussed above. Double layer forces may be quantified in terms of zeta potential (Johnson et al. 2000) rather than the more complicated techniques used in the numerical studies that have been discussed. It may be possible to obtain a closed form solution (or a table-style solution) using a simplified geometry such as the one discussed in the previous chapter and shown in Figure 14. This was attempted, but no logical way to quantify the magnitude of the positive surface charge on the edges of the platelets was found. The findings of this study indicate that this is a vital component of a theoretical model that would describe clay behavior.

REFERENCES

Anandarajah, A. (1994). “Discrete element method for simulating behavior of cohesive soil.” Journal of Geotechnical Engineering, ASCE, 120(9), 1593-1613

Anandarajah, A. (2000). “Numerical simulation of one-dimensional behavior of Kaolinite.” Geotechnique, 50 (5), 509-519

Anandarajah, A. and Chen, J. (1994). “Double-layer repulsive force between two inclined platy particles according to the Gouy-Chapman theory.” J. of Colloid and Interface Science, 168, 111-117

Anandarajah, A. and Chen, J. (1997). “Van der waals attractive force between clay particles in water and contaminants.” Soils and Foundations, Japanese Geotechnical Society, 37(2), 27-37

Archer, D. J. (1969). “X-ray diffraction of deep-sea clay minerals.” Ph.D. Thesis, University of Manchester

ASTM. (1989). “Standard test method for one-dimensional consolidation properties of soils using controlled-strain loading.” D 4186-89 (Re-approved 1998), PA

ASTM. (1996). “Standard test method for one-dimensional consolidation properties of soils.” D 2435-96, PA

Bennett, R. H. and Hurlbut, M. H. (1986). “Clay microstructure.” International Human Resources Development Corporation, Boston/Houston/London, 161

Brindley, G. W. and Robinson, K. (1946). “Randomness in the structures of kaolinite clay minerals.” Trans. Faraday Soc., 42b, 198-205

Casagrande, A. (1932). “The structure of clay and its importance in foundation engineering” Contributions to Soil Mechanics, 1925-1940, Boston Soc. of Civil Eng., Boston, 72-112

Chen, J. and Anandarajah, A. (1998). “Influence of pore fluid composition on volume of sediments in kaolinite suspensions.” Clay and Clay Minerals, 46(2), 145-152

Derjaguin, B. (1934). Kolloid-Z., 69(155)

Gibson, R. E., England, G. L., and Hussey, M. J. L. (1967). “The theory of one-dimensional consolidation of saturated clays.” Geotechnique, 17, 261-273

Gibson, R. E., Schiffman, R. L., and Cargill, K. W. (1981). “The theory of one-dimensional consolidation of saturated clays II. Finite nonlinear consolidation of thick homogeneous layers.” Can. Geotech. J., 18, 280-293

Gillot, J. E. (1970). “Fabric of leda clay investigated by optical, electron-optical, and x-ray diffraction methods.” Engineering Geology, 4(2), 133-153

Gorman, C. T., Hopkins, T. C., Deen, R. C., and Drnevich, V. P. (1978). “Controlled rate-of-strain and controlled gradient consolidation testing.” Geotechnical Testing Journal, 1(1), 3-15

Hazen, I., and Penumadu, D. (1999). “Resonant column testing of clay specimens with controlled microfabric.” Rep. No. 99-02, CEE Dept., Clarkson University, Potsdam, NY

Johnson, S. B., Franks, G. V., Scales, P. J., Boger, D. V., and Healy, T. W. (2000). “Surface chemistry-rheology relationships in concentrated mineral suspensions.” Int. J. Miner. Process., 58, 267-304

Lambe, T. W. (1958). “The structure of compacted clay.” J. Soil Mech. and Found. Div., ASCE, 84(SM2), Paper 1654, 1-34

Lee, K. (1981). “Consolidation with constant rate of deformation.” Geotechnique, 31(2), 215-229

Lee, K., Choa, S. H., and Quek, S. H. (1993). “Constant rate of strain consolidation of Singapore marine clay.” Geotechnique, 43(3), 471-488

Liu, M. D., Carter, J. P., and Desai, C. S. (2003). “Modeling compression behavior of structured geomaterials.” International J. of Geomechanics, 3(2), 191-204

Martin, R. T. and Ladd, C. C. (1974). “Fabric of consolidated kaolinite.” Clay and Clay Minerals, 23, 17-25

Mesri, G. and Choi, Y. K. (1985). “The uniqueness of the end-of-primary (EOP) void ratio-effective stress relationship.” Proc. 11^{th} Int. Conf. on Soil Mech. and Found. Eng., San Francisco, 2, 587-590

Mesri, G. and Feng, T. W. (1992). “Constant rate of strain consolidation testing of soft Clays.” Marsal Volume, Mexico City, 49-59

Mesri, G. and Olsen, R. E. (1971). “Mechanisms controlling the permeability of clays.” Clays and Clay Minerals, 19(3), 151-158

Mesri, G., Pakbaz, M. C., and Cepeda-Diaz, A. F. (1994). “Meaning, measurement and field application of swelling pressure of clay shales.” Geotechnique, 44(1), 129-145

Mesri, G. and Rokhsar, A. (1974). “Theory of consolidation for clays.” J. Geotechnical Engineering, ASCE, 100(8), 889-904

Mesri, G., Ullrich, C. R., and Choi, Y. K. (1978). “The rate of swelling of overconsolidated clays subjected to unloading.” Geotechnique, 28(3), 281-307

Mitchell, J. K. (1956). “The fabric of natural clays and its relation to engineering Properties.” Proc. High. Res. Bd., 35, 693-713

Mitchell, J. K. (1993). Fundamentals of Soil Behavior

Penumadu, D. (1996). “Evaluating clay microfabric using scanning electron microcopy and digital information processing.” Transp. Research Rec., TRB, 1526, 112-120

Penumadu, D., Skandarajah, A., and Chameau, J.-L. (1998). “Strain-rate effects in pressuremeter testing using a cuboidal shear device: experiments and modeling.” Can. Geotech. J., 35, 27-42.

Pestana, J. M. and Whittle, A. J. (1999). “Formulation of a unified constitutive model for clays and sands.” Int. J. Numer. and Anal. Meth. in Geomech., 23, 1215-1243

Pestana, J. M., Whittle, A. J., and Gens, A. (2002). “Evaluation of a constitutive model for clays and sands: Part II – clay behavior.” Int. J. Numer. and Anal. Meth. in Geomech, 26, 1123-1146

Quigley, R. M. and Thompson, C. D. (1966). “The fabric of anisotropically consolidated sensitive marine clay.” Canadian Geotechnical J., 3, 61-73

Roscoe, K. H. and Burland, J. B. (1968). “On the generalized stress-strain behavior of ‘wet’ clay.” Engineering Plasticity (J. Heyman and F. A. Leckie, eds), Cambridge University Press, 535-609

Sachan, A. and Penumadu, D. (2004). “Identification of microfabric of kaolin clay using x-ray diffraction technique.” ASTM Goetechnical Testing Journal, in review, submitted September, 2004

Sällfors, G. (1975). “Preconsolidation pressure of soft, highly plastic clays.” Chalmers University of Technology, Goteborg, Sweden

Sheahan, T. C. and Watters, P. J. (1996). “Using an automated Rowe cell for constant rate of strain consolidation testing.” Geotech. Test. J., 19(4), 354-363

Sheahan, T. C. and Watters, P. J. (1997). “Experimental verification of CRS consolidation theory." J. Geotechnical and Geoenvironmental Engineering, ASCE, 123(5) 430-437

Smith, R. E., and Wahls, H. E. (1969). "Consolidation under constant rate of strain." J. Soil Mech. and Found. Div., ASCE, 95(SM2), 519-539

Terzaghi, K. (1941). "Undisturbed clay samples and undisturbed clays." Journal of the Boston Society of Civil Engineers, 28(3), 211-231

Terzaghi, K., Peck, R. P., and Mesri, G. (1996). Soil Mechanics in Engineering Practice

Verwey, E. J. W. and Overbeek, J. Th. G. (1948). "Theory of the stability of lyophobic colloids." Elsevier, Amsterdam, New York, London

Whittle, A. J. (1993). "Evaluation of a constitutive model for overconsolidated clays." Geotechnique, 43(2), 289-313

Whittle, A. J. and Kavvadas, M. (1994). "Formulation of the MIT-E3 model for overconsolidated clay." J. Geotechnical Engineering, ASCE, 120(1), 173-198

Winterkorn, H. F. and Tschebotarioff, G. P. (1947). "Sensitivity of clay to remolding and its possible causes." Proc. Highway Research Board, 27

Wissa, A. E. Z., Christian, J. T., Davis, E. H., and Heiberg, S. (1971) "Consolidation at a constant rate of strain." J. Soil Mechanics and Foundations Division, ASCE, 97(SM10) 1393-1413

Yao, M. and Anandarajah, A. (2003). "Three-dimensional discrete element method of analysis of clays." J. of Engineering Mechanics, ASCE, 129(6), 585-596

APPENDIX 1: TABLES AND FIGURES

Table 1: Settling Column Test Results		
	e_o	e_f
Slurry Prepared Without Dispersing Agent 1	4.07	**3.76**
Slurry Prepared Without Dispersing Agent 2	4.07	**3.77**
Slurry Prepared With Dispersing Agent 1	4.07	**1.58**
Slurry Prepared With Dispersing Agent 2	4.07	**1.59**
Slurry Prepared Without Dispersing Agent (double initial water content)	8.14	**5.01**

Table 2: Summary of Effects of Dispersing Agent on Slurry Properties						
			Viscosity (Pa-s)			
	pH	Zeta Potential (mV)	at 30 s^-1	at 60 s^-1	at 90 s^-1	Liquid Limit
Without Dispersing Agent	4.6	-44.4	1.8	1.4	1.1	59
With Dispersing Agent	6.1	-48.7	0.017	0.013	0.011	32

Table 3: Summary of Leeching Tests Under Applied Vertical Stress					
	Void Ratio				
Ultimate Applied Vertical Stress	Initial	Under Applied Stress	Under Applied Stress After Leeching	Average Value for Samples Prepared with a Dispersing Agent Under the Same Vertical Effective Stress	Degree of Dispersion
(kPa)	e_o	e_l	e_f	e_d	
0	8.14	5.01	2.45*	1.59	0.75*
98.3	1.163	1.086	0.811	0.669	0.66
272.6	1.175	1.054	0.776	0.603	0.62
498.6	1.183	0.904	0.707	0.559	0.57
988.5	1.194	0.795	0.694	0.5	0.34

*At the time of the submission of this thesis, the sediment had not yet stabilized. The reported value is that which was reached at the time of submission. The value for degree of dispersion is increasing with time.

Table 4: Virgin Compression and Swelling Indexes			
	Cc	***Cs***	e_o
Vertical Samples with Flocculated Micro-Fabric			
IL VF01	0.39	0.073	1.181
IL VF02	0.40	0.066	1.160
CRS VF03	0.38	0.076	1.110
CRS VF04	0.38	0.059	1.193
CRS VF05	0.37	0.060	1.168
average	**0.385**	**0.067**	**1.162**
standard deviation	0.011	0.008	0.032
Horizontal Samples with Flocculated Micro-Fabric			
IL HF01	0.35	0.064	1.152
CRS HF02	0.32	0.037	1.144
CRS HF03	0.35	0.043	1.158
CRS HF04	0.35	0.036	1.163
CRS HF05	0.35	0.045	1.181
CRS HF06	0.34	0.046	1.175
average	**0.344**	**0.045**	**1.162**
standard deviation	0.014	0.010	0.014
Vertical Samples with Dispersed Micro-Fabric			
IL VD01	0.18	0.074	0.742
CRS VD02	0.17	0.064	0.781
CRS VD03	0.18	0.056	0.770
CRS VD04	0.18	0.064	0.781
CRS VD05	0.20	0.067	0.789
average	**0.181**	**0.065**	**0.773**
standard deviation	0.013	0.007	0.018
Horizontal Samples with Dispersed Micro-Fabric			
IL HD01	0.17	0.056	0.757
CRS HD02	0.18	0.047	0.787
CRS HD03	0.17	0.047	0.773
CRS HD04	0.16	0.045	0.767
average	**0.173**	**0.049**	**0.771**
standard deviation	0.007	0.005	0.013

Table 5: Degrees of Anisotropy			
Micro-Fabric	Degree of Anisotropy	Elastic Degree of Anisotropy	Plastic Degree of Anisotropy
Flocculated	0.11	0.32	0.06
Dispersed	0.045	0.25	-0.07

Table 6: Degrees of Plasticity		
Micro-Fabric	Direction of Loading	Degree of Plasticity
Flocculated	Vertical	0.83
	Horizontal	0.87
Dispersed	Vertical	0.64
	Horizontal	0.72

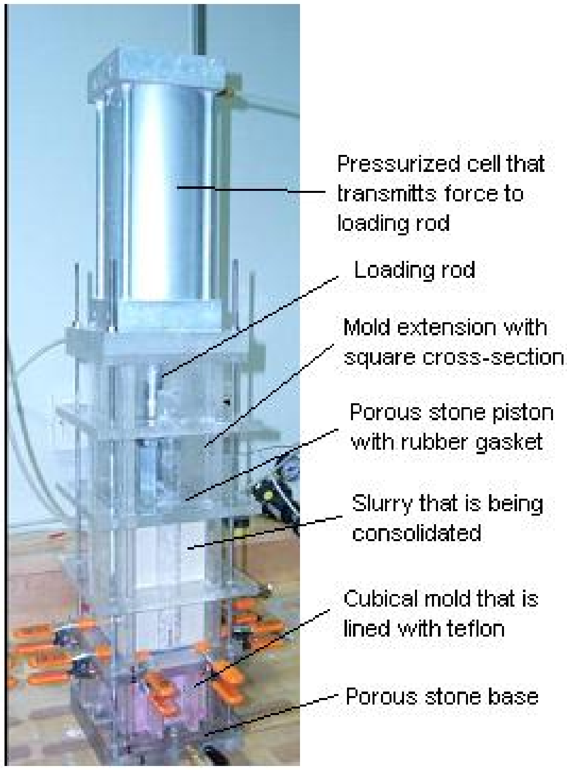

Figure 1: Consolidometer and Extruded Cubical Specimen

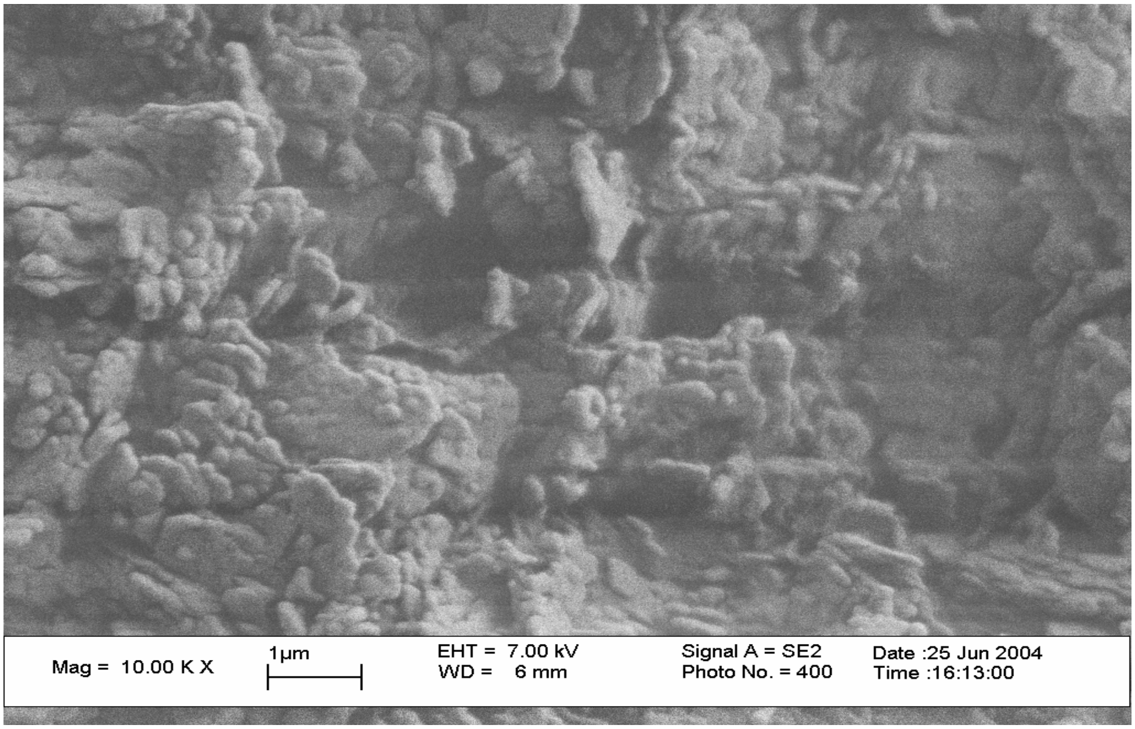

(a)

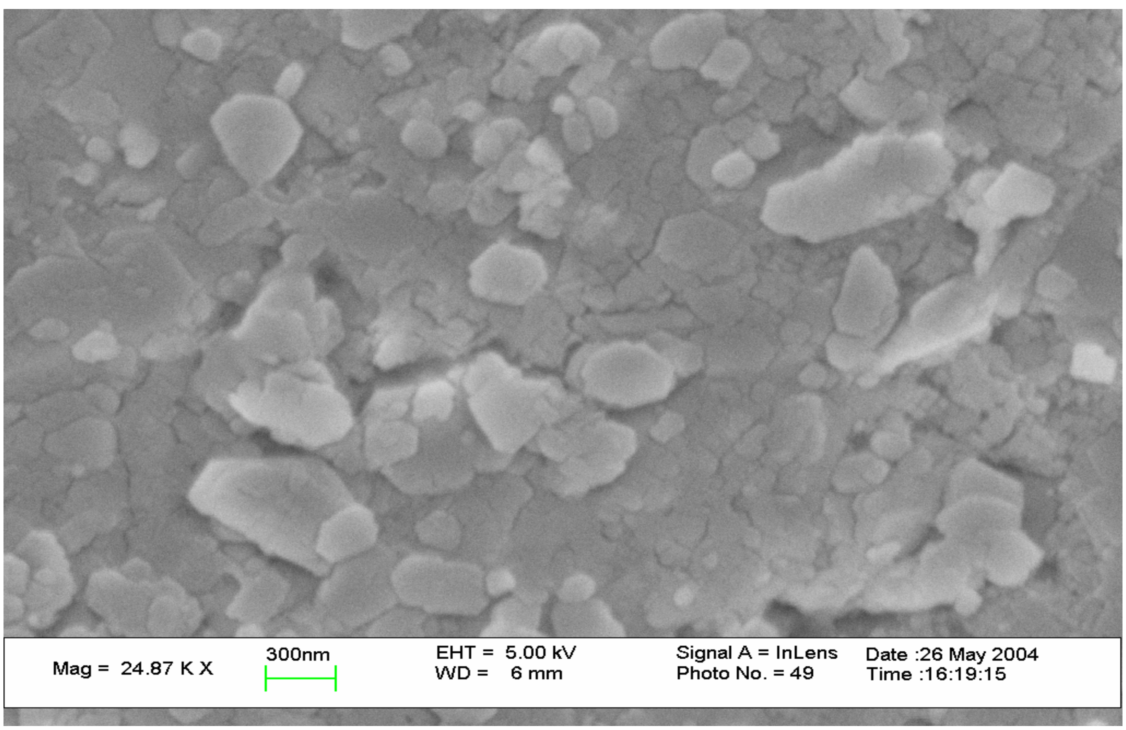

(b)

Figure 2: SEM Image of Air-Dried Sediment from Kaolin Clay Slurry Prepared (a) without a Dispersing Agent (10,000x) and (b) with a Dispersing Agent (25,000x)

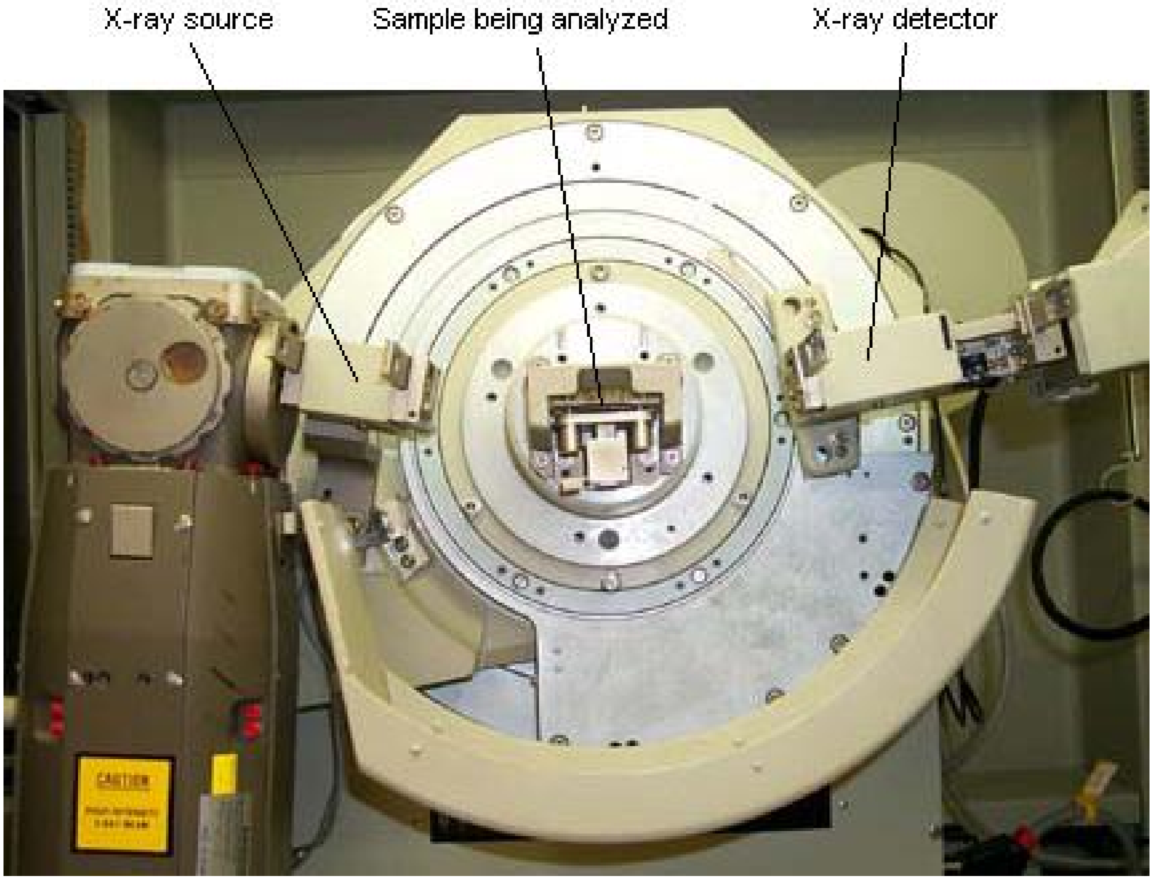

Figure 3: Siemens Diffractometer model D500

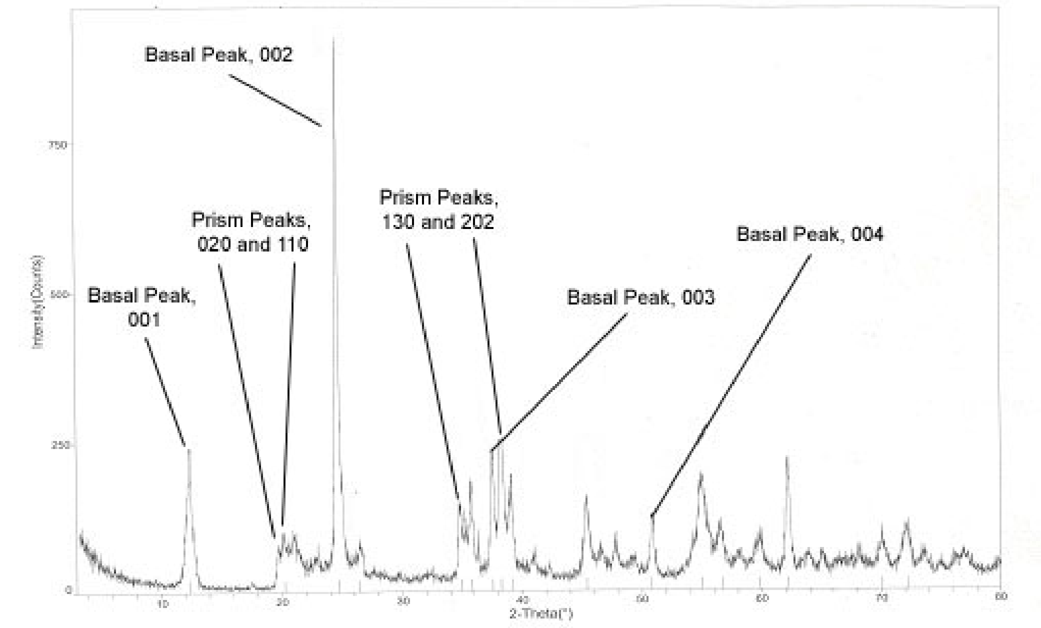

(a)

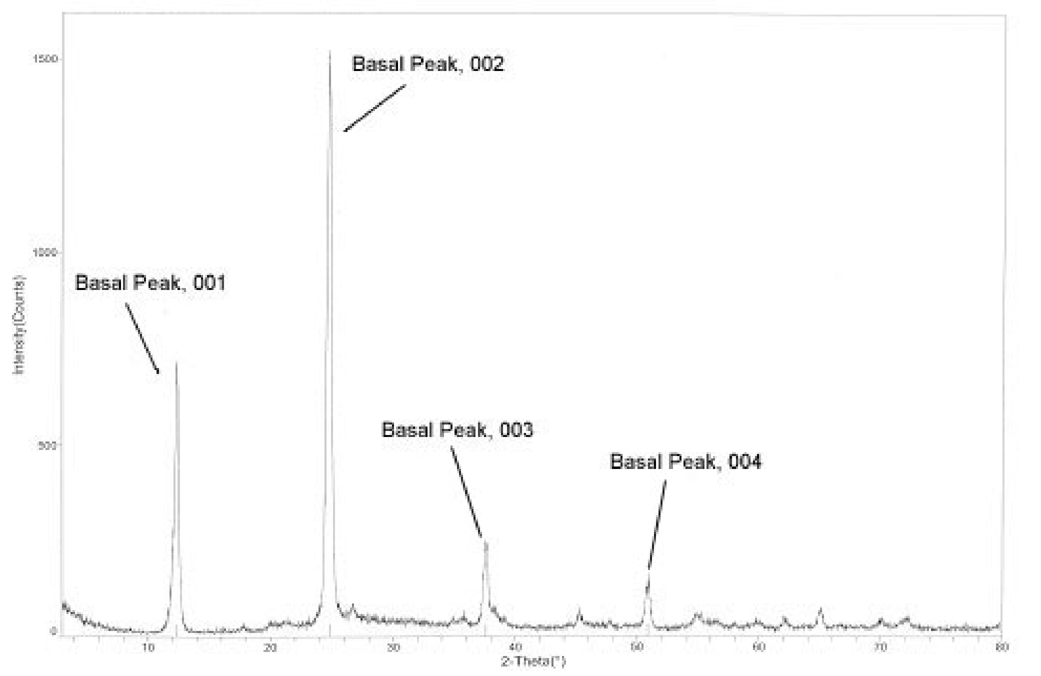

(b)

Figure 4: X-ray Diffraction Pattern for Air-Dried Sediment from Kaolin Clay Slurry Prepared (a) without a Dispersing Agent and (b) with Dispersing Agent

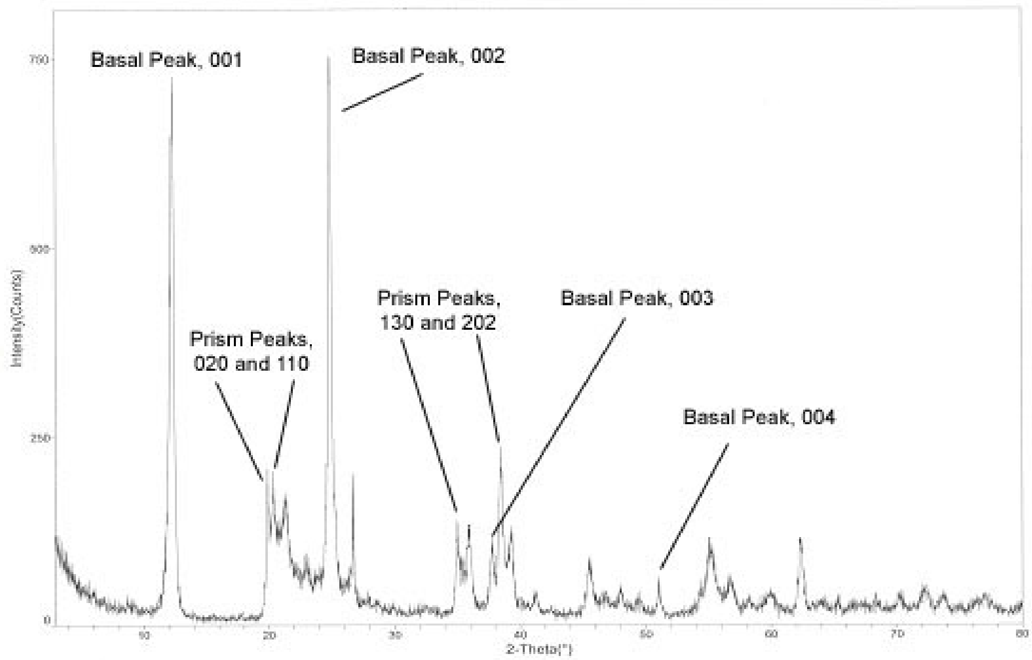

(a)

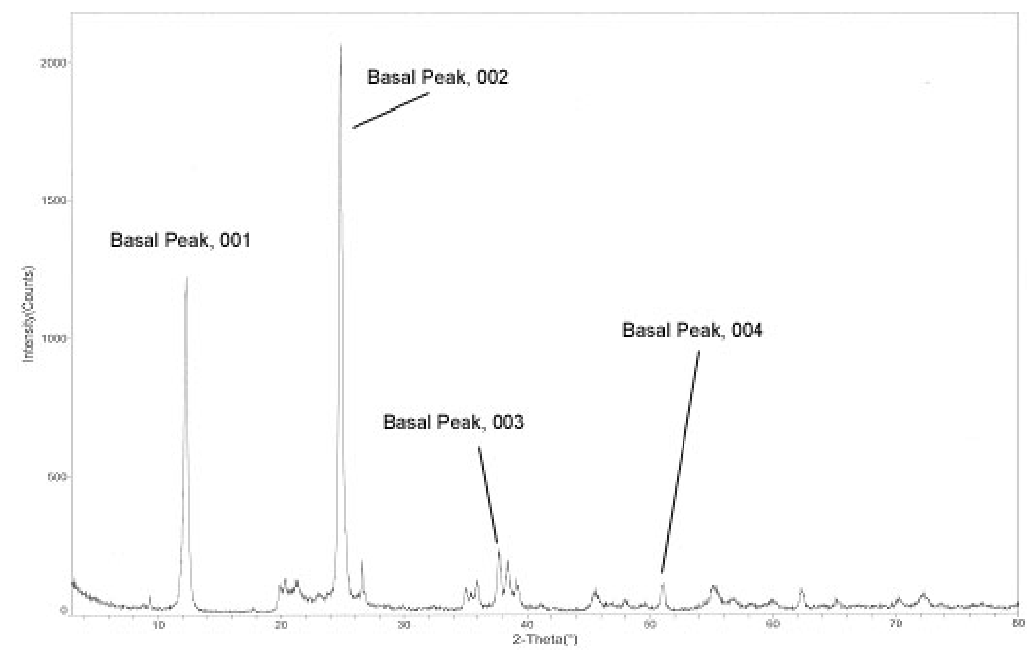

(b)

Figure 5: X-ray Diffraction Pattern for One-Dimensionally Consolidated (Preconsolidation Stress = 30 psi) Kaolin Clay Sample with (a) Flocculated Micro-Fabric and (b) Dispersed Micro-Fabric

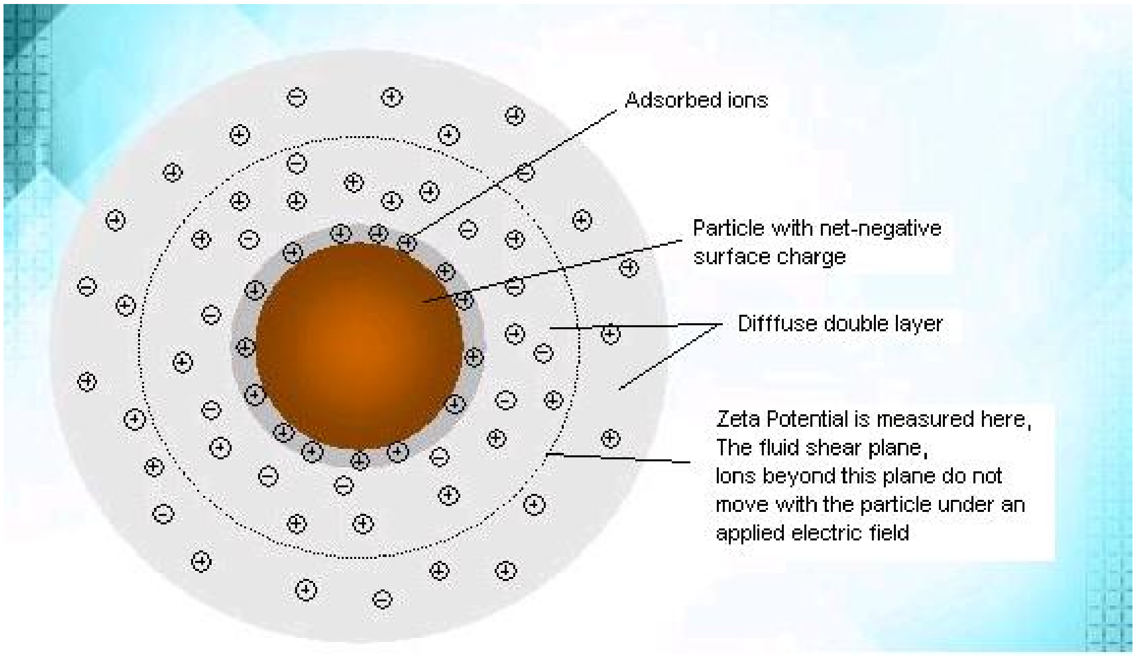

Figure 6: Diagram Explaining the Concept of Zeta Potential

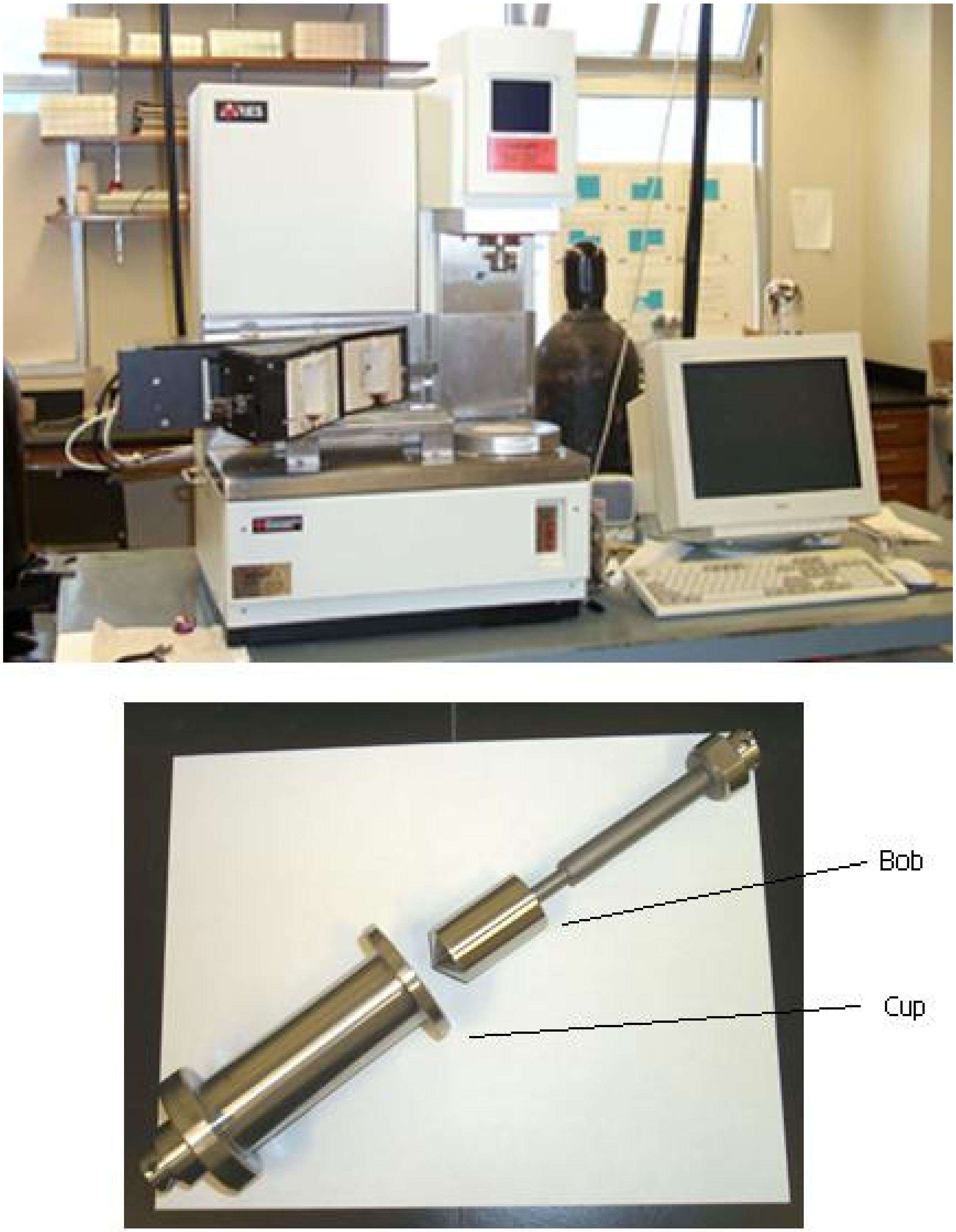

Figure 7: Rheology Testing Apparatus and Cup and Bob Geometry

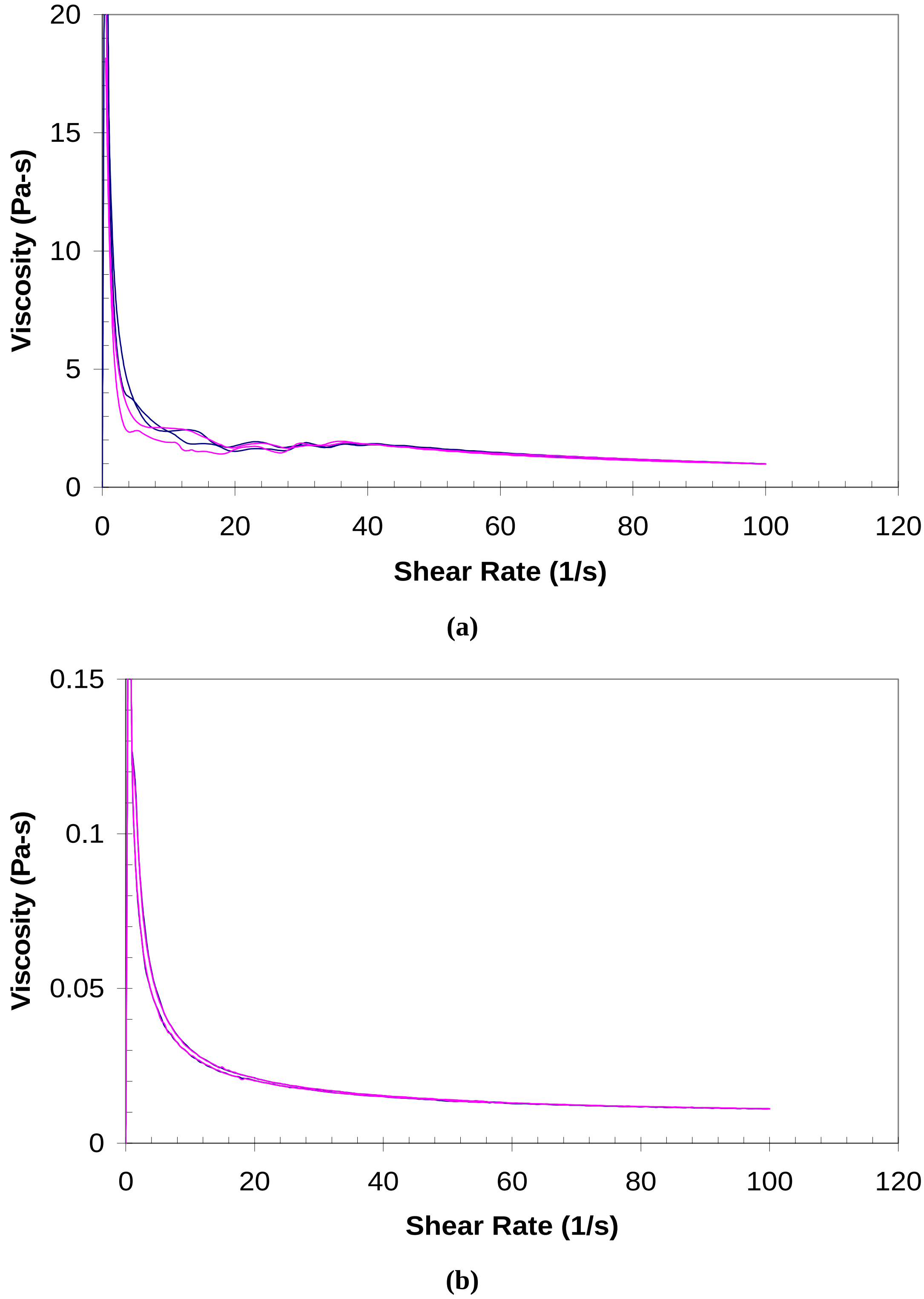

Figure 8: Rheology Test Results as a Function of Shear Rate for Kaolin Clay Slurry Prepared (a) without a Dispersing Agent and (b) with Dispersing Agent

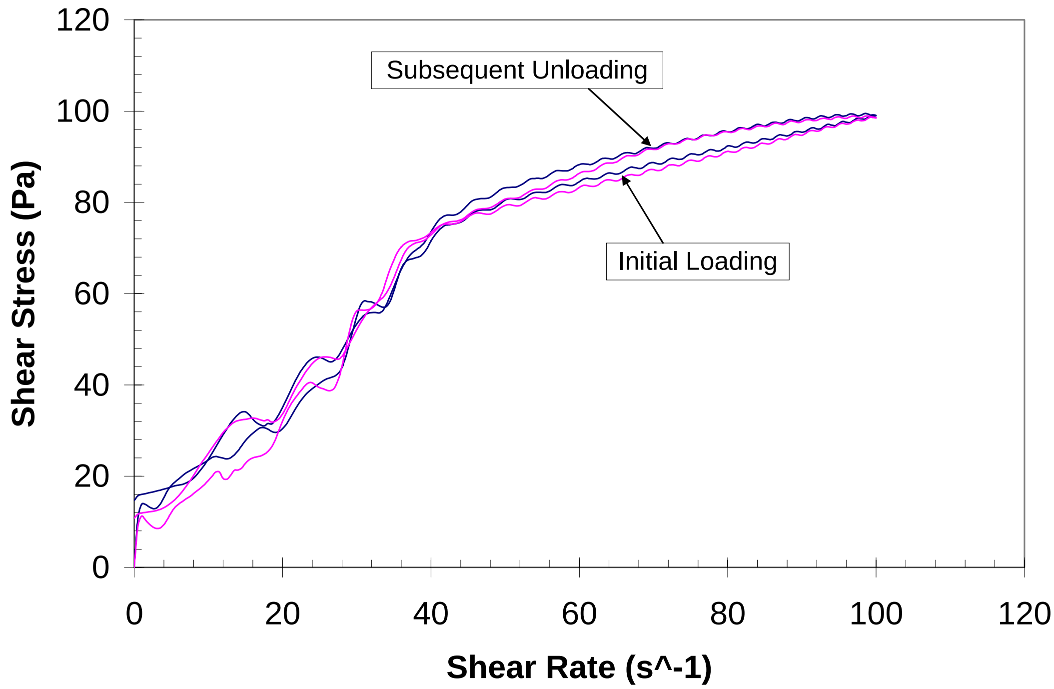

(a)

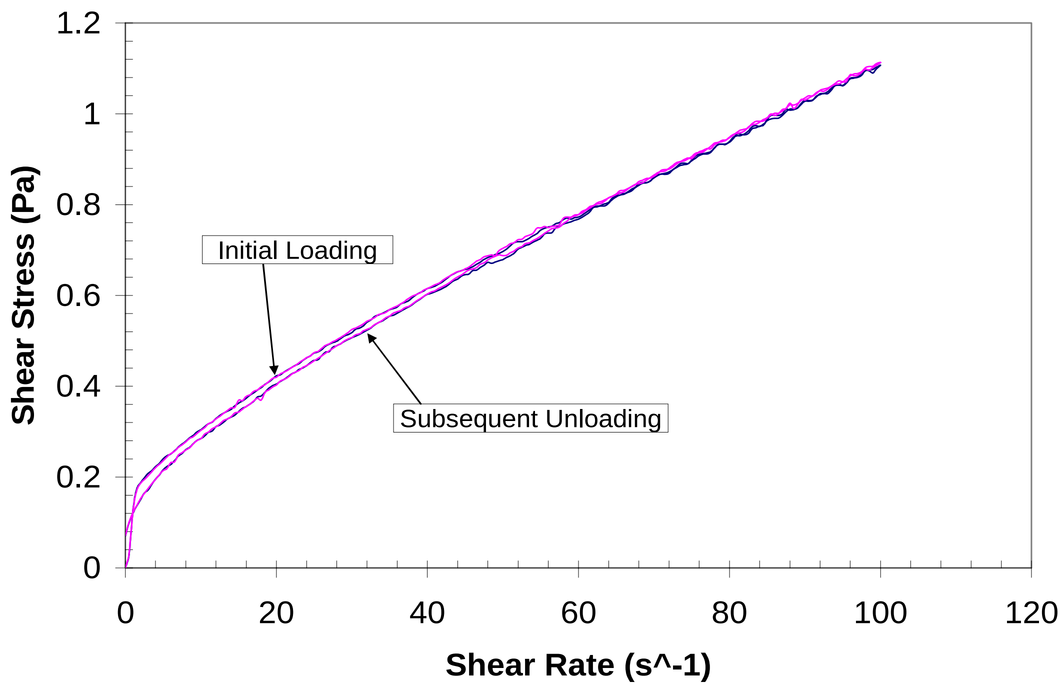

(b)

Figure 9: Shear Stress as a Function of Applied Shear Rate for Kaolin Clay Slurry Prepared (a) without a Dispersing Agent and (b) with Dispersing Agent

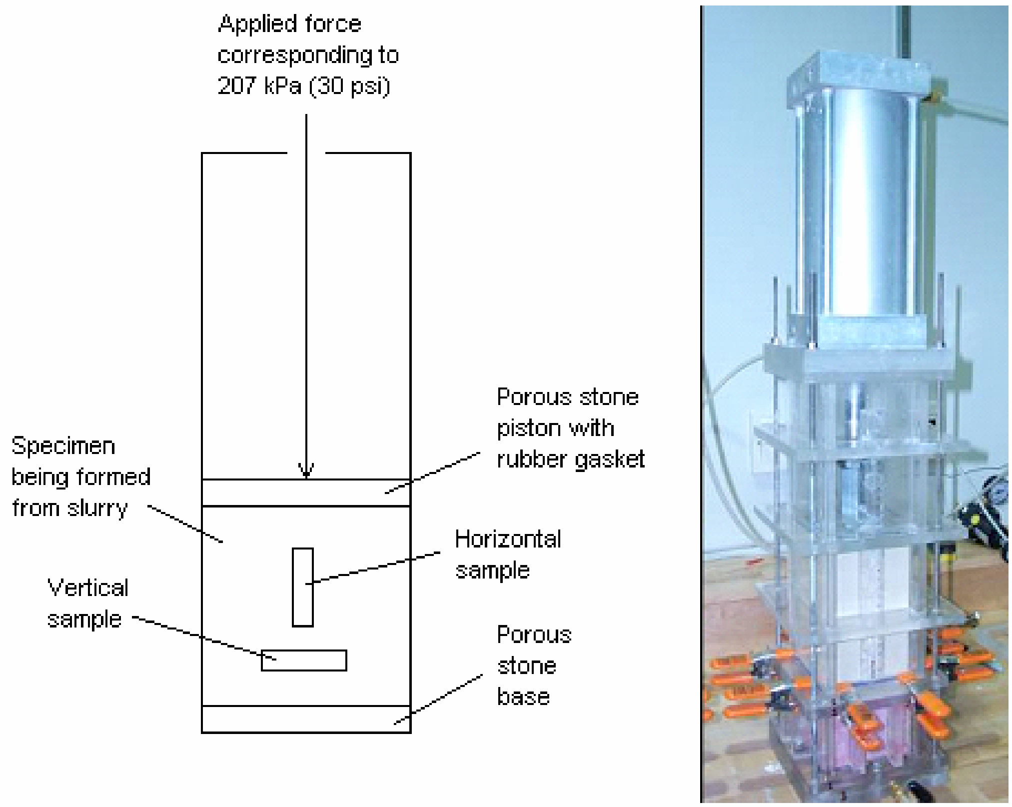

Figure 10: Diagram Explaining Orientation of Consolidation Test Samples Relative to their Orientation in the Consolidometer during Specimen Preparation

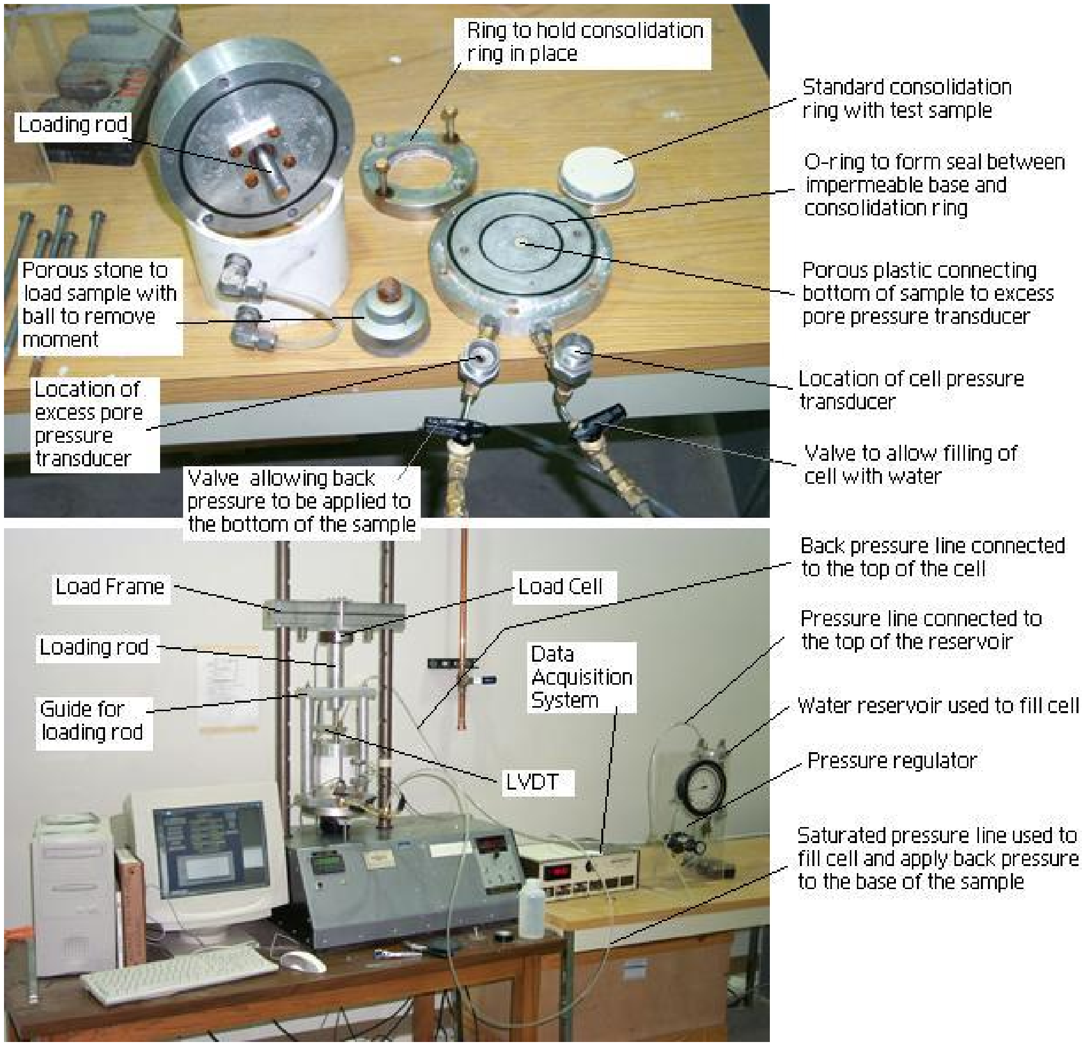

Figure 11: Disassembled Cell and Controlled-Rate-of-Strain (CRS) Consolidation Testing Apparatus with Computer and Data Acquisition System

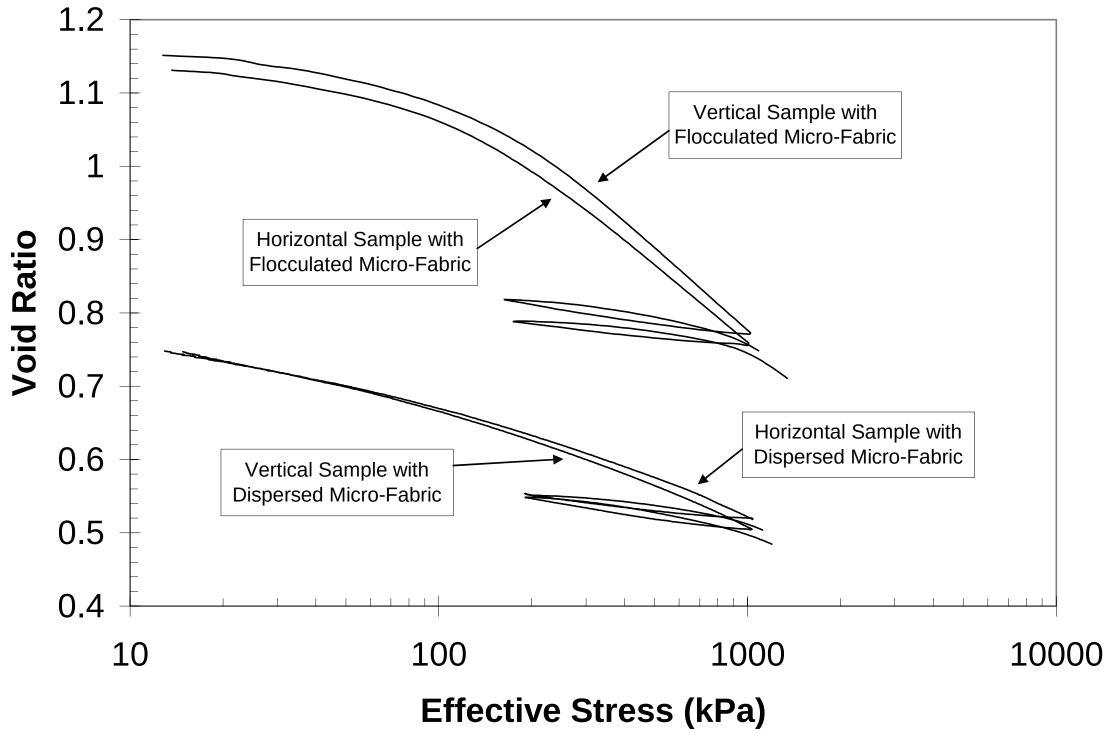

Figure 12: Representative One-Dimensional Consolidation Curves for Vertical and Horizontal Kaolin Clay Samples with Flocculated and Dispersed Micro-Fabric

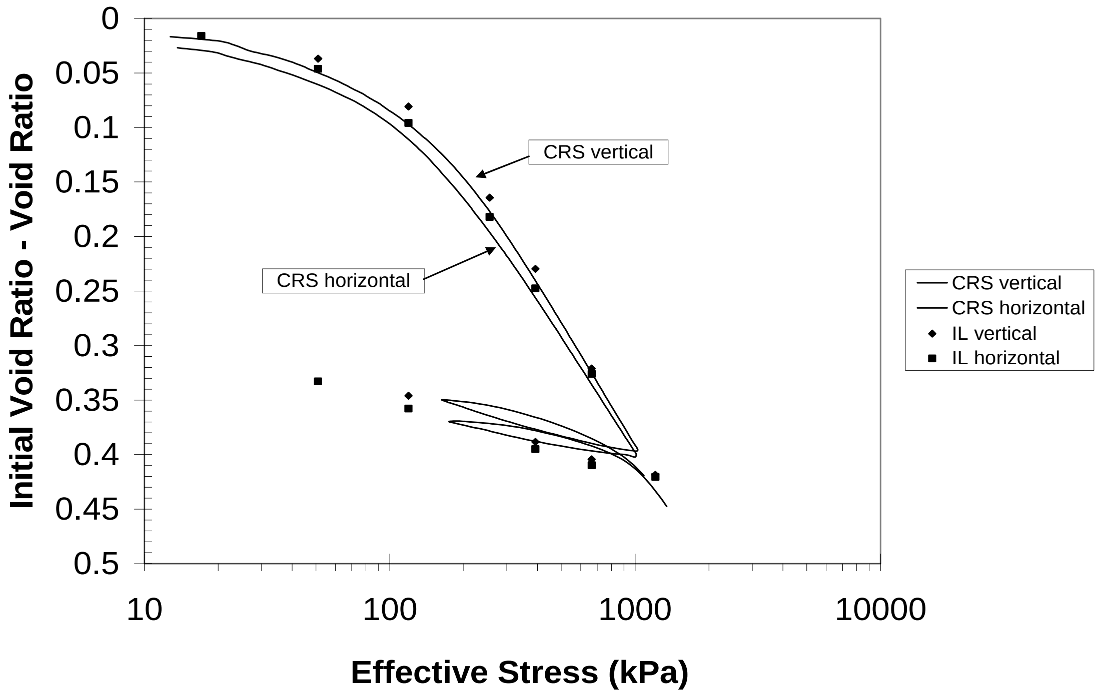

(a)

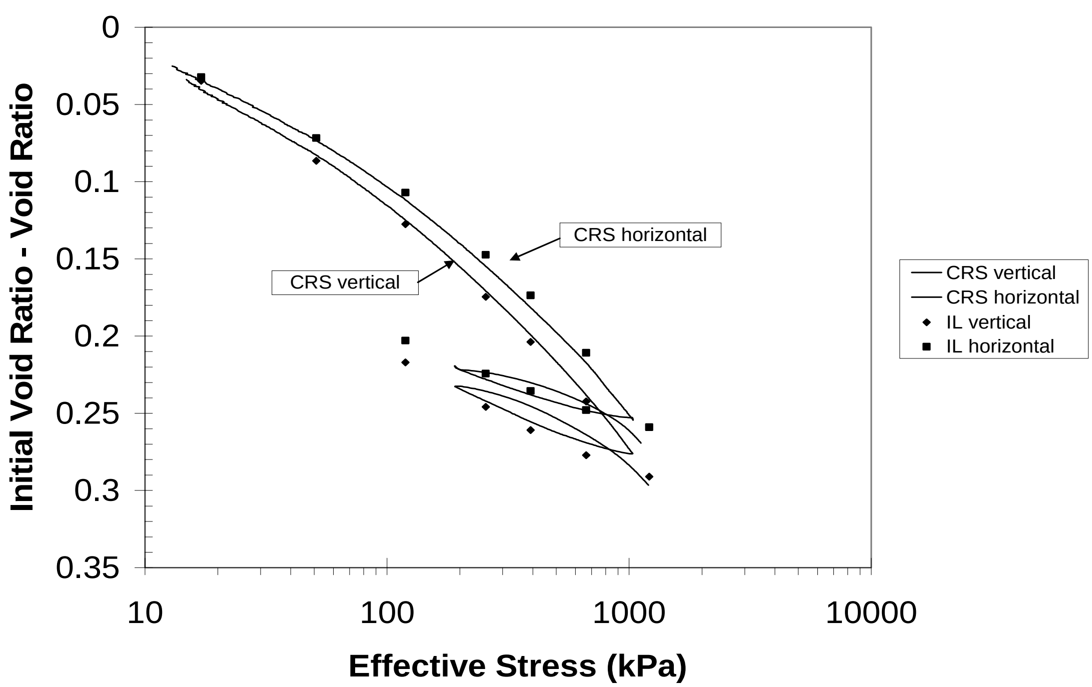

(b)

Figure 13: Comparison between CRS and IL Consolidation Test Results for (a) Flocculated Micro-Fabric and (b) Dispersed Micro-Fabric

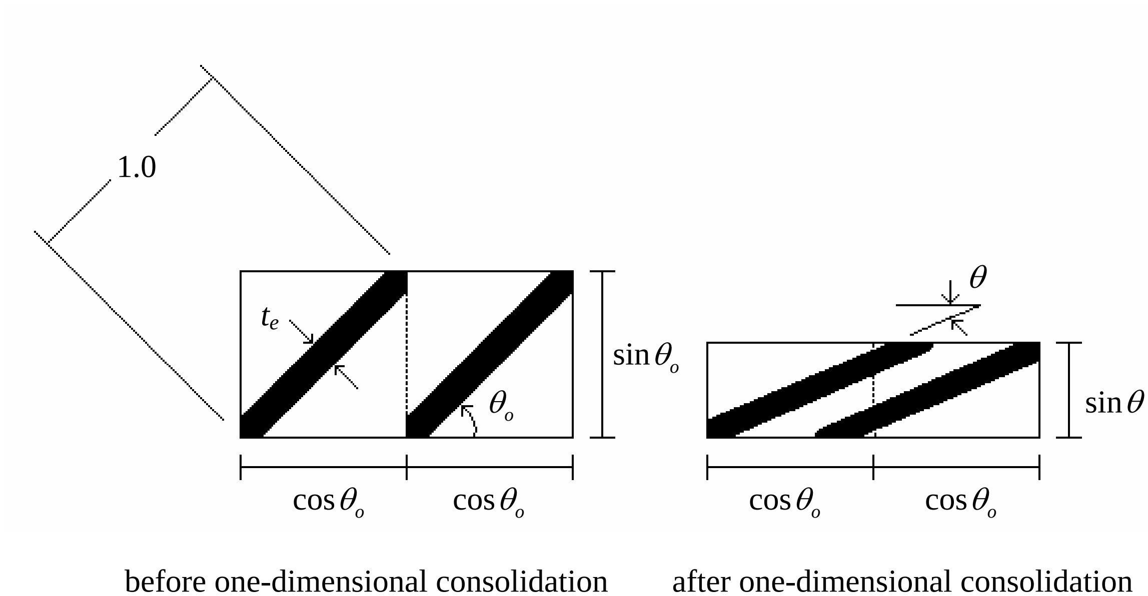

Figure 14: Geometric Model Used to Obtain Effective Thickness (t_e) and Average Platelet Orientation Angle (θ) as a Function of Void Ratio

Vita

Alex Davis-Smith was born in Nashville, TN on May 28, 1980. He went to high school at Hillsboro High School and graduated in 1998. He then attended the University of Tennessee in Chattanooga for one year before transferring to the University of Tennessee in Knoxville. He received a B.A. in civil engineering in 2002 and an M.S. in civil engineering in 2004.